Monitoring of Forest Biodiversity Using Remote Sensing: Forest Stand (High Spatial Resolution) Protocol and Examples

Elizabeth E. Dickson, Steven E. Franklin, and L. Monika Moskal
Department of Geography, University of Calgary, 2500 University Dr. NW, Calgary, T2N 1N4
Eedickso@ucalgary.ca;

March 1999

Disclaimer
The views, statements, and conclusions expressed in this report are those of the authors and should not be construed as conclusions or opinions of the ABMP. Development of the ABMP has continued during the time since this report was produced. Thus, the report may not accurately reflect current ideas.

Introduction

The Alberta Forest Biodiversity Monitoring Program (AFBMP) remote sensing pilot project, is aimed at developing protocols for monitoring forest biodiversity using multi-resolution remotely sensed data. Ultimately, the protocols for remote sensing will be integrated with protocols developed in parallel pilot projects for taxonomic groups and ecosystems representing the diversity of the province, i. e., mammals, birds, arthropods, terrestrial plants and bryophytes, and aquatic systems.

This chapter is derived from a second report of the AFBMP remote sensing pilot study, providing an initial protocol for using high spatial resolution imagery (< 2 m per pixel) to monitor stands on the forested landscape. It follows an earlier report on remote sensing protocols for forested regional landscape using low spatial resolution imagery (Chapter 8).

Scale

Biodiversity and Scale

Biodiversity is multi-dimensional in character, involving multiple species and ecological processes that interact and proceed at multiple scales (Noss 1998). According to hierarchy theory, temporal and spatial scales covary; longer processes tend to occur over larger spaces. Sampling biodiversity at more than one spatial scale allows a more complete understanding of simultaneously existing processes that operate on different time scales. In this context, the magnitude of the study (area and time) and the degree of detail collected can be adjusted purposefully to capture the level of biodiversity sought.

In practice, tradeoffs exist between the level of detail and the amount of area that can be examined. The level of detail that can be extracted in large areal units is generally smaller due to practical considerations, such as time, transportation, field crew expense, and analyzing samples. For the same time and effort, greater detail can be collected from smaller areas, increasing the probability of detecting subtle changes in species composition or ecological processes.

As pointed out in Chapter 8, measures of landscape pattern that are important biodiversity elements in their own right, are dependent on the areal extent that is tested. Decisions remain outstanding regarding the size or sizes of area chosen for long-term biodiversity monitoring. If detection and intensity of change is dependent on sample area, choosing the level of environmental change that signals consequential shifts in biodiversity is first required before the extent of the sample area can be decided.

Remote Sensing and Resolution

For studies using remotely sensed data, spatial scale has the same meaning as in ground-based studies; the areal extent of the investigation. The level of spectral and spatial detail that can be collected remotely, however, is determined by the resolution capabilities of the sensor. Therefore, information that can be derived from remotely sensed imagery, which includes land composition (type of patches) and pattern, will vary according to the sensor used. See Chapter 7 for a more thorough discussion of resolution and remote sensing.

By including information derived from multiple resolutions of remotely sensed data in a monitoring program, a broad measure of the multi-dimensionality of biodiversity will be obtained. Besides enhancing measures of biodiversity, these dimensions will add to our general understanding of how the composition and pattern of the landscape at different spatial resolutions are related to one another. For these reasons, a multi-resolution approach to biodiversity monitoring is recommended.

For low spatial resolution imagery such as satellite Landsat TM (30 m/pixel), usually more than one type of ground object occupies the space corresponding to a single pixel. In this case, the sensor detects a mixture of spectral reflectance from underlying ground objects. Each object's spectral signature contributes to the pixel's overall signature in proportion to its fraction on the ground. Information extracted from low spatial resolution imagery is limited to broadly defined classes that often include more than one plant species, rock type, urban structure or other ground object form. The pixel-based approach to classification is commonly used with low spatial resolution imagery, which assumes pixel independence and signatures based on normal distributions of pixel multispectral values.

In contrast, for high spatial resolution imagery, a single ground object may correspond to more than one pixel. In addition, pixels comprising a single ground feature may vary in spectral properties. For example, different parts of a tree can vary in reflectance properties, depending on illumination conditions (sun or shade) and biochemical (photosynthetic) activity (leaf or bark). Therefore, one important aspect of extracting information from high spatial resolution data is object identification and definition; that is, determining the set of contiguous pixels that belong to a certain ground feature.

Biodiversity Elements

Components of forest structure and composition provide a basis for habitat mapping, forest diversity indices (Lahde et al. 1999) and studies of ecological processes. Forest structure refers to the vertical and horizontal organization of above ground plant matter, varying from uniform even-aged stands to irregular multiple-aged mixed stands. For forestry and ecological applications, vegetation structure can be categorized as inventory information (tree stem counts, standing and fallen dead trees, charred wood, crown closure, canopy height, canopy and understory species composition) or as biophysical parameters (LAI, biomass, NPP) (Wulder 1999 says '99 in references). Some of these components are the types of biodiversity elements that can be monitored within a forest stand using medium and high spatial resolution remotely sensed data. A list of recommended biodiversity elements for monitoring forest stands using medium and high spatial resolution data is given in Table 9.1.

Table 9.1 Selected Biodiversity Elements – Medium and High Spatial Resolution Imagery

Biodiversity Element	Method
Species Composition	Object Detection and Classification
Number of Trees	Object Detection and Classification
Canopy Roughness	Classification and Texture
Crown Closure	Object Detection and Classification
Vegetation Index	Image Algebra
Vegetation Stress	Linear Models (Regression)
Leaf Area Index	Linear Models (Regression)
Canopy Volume	Linear Models (Regression)
Patch (Gap) Metrics	Metric and Spatial Algorithms

A number of recent studies have addressed the effectiveness of high spatial resolution satellite and airborne imagery to determine various components of vegetation structure and composition. A brief review of the remote sensing literature addresses selected biodiversity elements (Table 9.1). Following the review, examples are provided that show graphic illustration of biodiversity elements extracted from medium and high spatial resolution airborne data using data collected from the AFBMP's Foothills and Boreal Pilot Areas and from the Kananaskis Biological Field Station, University of Calgary.

Literature Review

Species Classification

A pixel-based approach to classifying high spatial resolution Digital Multispectral (DMS) images (25 cm x 32 cm pixel resolution) of a forested region in the foothills of Alberta was compared to ground-based class information (Gerylo et al. 1998). Using pixels corresponding to sunlit tree crowns, spectral signatures of pure species were delineated as training sets for a maximum likelihood classifier. For accuracy assessment, a tree crown mask was utilized, eliminating classification error from the understory. An average class accuracy of 84% resulted for lodgepole pine, white spruce and aspen; improving to 89% by combining the two conifer classes. From 66% overall accuracy for the three tree species classes, the overall accuracy decreased significantly when more classes were included in the analysis (Gerylo et al. 1998).

Through empirical studies, texture derivatives of high spatial resolution (< 2 m/pixel) images by and large have shown improvements to canopy classification accuracy using pixel-based classifiers (Dikshit and Roy 1996; Franklin et al. 1999). The incorporation of texture information improved discrimination between eight texture-based classes (water, fen reed, fen *Phalaris*, wet grass, wet grass (mowed or grazed), fen herbs, sallow scrub, and woodland) in an aerial image (1.25 m/pixel) taken near Cambridge, UK (Dikshit and Roy 1996). Using Compact Airborne Spectrometric Imager (*CASI*) data with spatial resolutions less than 1 m/pixel, Franklin et al. (2000) found that homogeneity and entropy texture derivatives slightly improved pure and mixedwood forest class accuracy in Alberta (60% to 65%). The same study showed that accuracy improved with texture derivatives by 12% for forest classes in New Brunswick (Franklin et al. 2000).

However, pixel-based approach to classifying species has not proven to be highly effective using high-resolution imagery (Gerylo et al. 1998). Pixels within the same tree can end up being classified differently using a pixel-by-pixel method, complicating errors. To avoid this problem, classifications can be performed using groups of pixels that represent individual trees or groups of trees.

Brandtberg (1998) developed two methods for distinguishing tree species in Swedish forests (*Picea abies*, *Pinus silvestris*, and *Betula* spp.) based strictly on tree crown patterns. By using filtered aerial infrared imagery (10 cm/pixel), a radial measure could discriminate undamaged spruce tree crowns and a contour measure of the crowns of pine and birch. Spruce crowns are characterized by rows of brighter pixels radiating out from a central core, while the smooth contour of a birch crown is distinctive from the curved contour of a pine crown (Brandtberg 1998).

In early work with high resolution Multidetector Electro-optical Imaging Scanner (MEIS) imagery (36 cm/pixel), tree crowns were delineated by hand (Gougeon 1995a). The spectral variability of sets of pixels within tree crowns was evaluated for use as signatures in classification: all pixels, sunlit pixels and shaded pixels. For five conifer species (black spruce, white spruce, jack pine, red pine, and white pine) and 10 classifications schemes, the average mean species classification accuracy ranged between 48.1% and 88.9%, with sunlit signatures performing the worst (Gougeon 1995a). Automated methods for delineating tree crowns are advancing (Gougeon 1995b; Gougeon et al. 1998) with application for estimating tree number, crown closure, etc. (see below), as well as classification. The individual tree crown (ITC) method of classification depends on highlighting the shaded areas among crowns on the image, delineating trees and clusters of trees (Gougeon et al. 1998). A supervised approach is taken using training sets from delineated tree crowns to gather spectral signatures of pure species. Maximum likelihood decision rules then place unknown ITC into species groups.

To classify high resolution (2 m/pixel), multi-spectral DMSV imagery, Preston et al. (1998) utilized a tree identification and delineation algorithm (TIDA) to search for distinct spectral patterns in a scene of Australian forest. Maximally and minimally bright pixels were used to identify crown centroids and boundaries on the imagery. This information was combined with environmental and field data for decision tree modeling and classification with intelligent algorithms. Compared to manual interpretation, the automated procedures were 20% more reliable overall (28% for species; 21% for size and density, 20% for tree development index, and 8% for height) (Preston et al. 1998).

In contrast to the methods above, an approach that does not delineate trees was tested for classifying species of deciduous trees. Images taken on ten separate occasions during a single year, documented phenological differences that proved to be useful for discriminating four deciduous tree species within an Appalachian mixed hardwood site (Key et al. 1998). Different combinations of spectral bands taken from the ten multi-date images were classified and compared for classification accuracy using a maximum likelihood classification algorithm. The authors concluded that the classification accuracy of the different band combinations depended on the species and on temporal and phenological resolution (Key et al. 1998).

Number of Trees

Four fundamental techniques have been developed and/or combined for estimating the number of trees per stand (stem density): 1) local maxima; 2) valley following; 3) template matching; and 4) edge contours at multiple scales.

The local maxima approach identifies and flags the brightest pixels among clusters of pixels within an image, corresponding to the reflectance off the highest point of the tree crown. For a conifer with a conical canopy, often only one highest point exists; for a deciduous tree with a spreading canopy, more than one brightest point may occur. By counting the number of flagged pixels, the number of trees within an image can be estimated. Similar to manual interpretation, 55% of the true number of conifer stems was estimated in different densities of even-aged Norway spruce stands by determining the maxima value above the mode of a smooth aerial photo (15 cm/pixel) (Dralle and Rudemo 1996). For determining the maxima by kernel smoothing, the band width of the imagery was found to be an important parameter. Later, Dralle and Rudemo (1997) extended an analysis of their study area, modifying the amount of image smoothing and comparing stem count estimates to ground counts. For estimating tree position from imagery, the authors showed reasonable results, 85%-95% of the trees are found with a RMSE of 65 cm (Dralle and Rudemo 1997). Using panchromatic orthophotos (1 m/pixel) of a conifer forest, the highest reflectance values were identified within the image via a moving window (Niemann et al. 1998). For tree top identification, the local maxima method corresponded by 70% to 85% to manual photo-interpretation (Niemann et al. 1998). The local maxima method is more successful at detecting individual trees in dense conifer stands where every tree is surrounded by shade, compared to thin stands where understory can cause false positives (Gougeon1997). For this reason, the local maxima algorithm was modified to account for the presence of a specific shadow for every tree with encouraging results (Gougeon 1997). Eldridge and Edwards (1993) estimated the number of stems/ha using MEIS-II (40 cm/pixel) imagery and a peak finding algorithm (local maxima filter). Extending the work of Eldridge and Edwards (1993), their algorithm was modified to identify individual stems in a mixed-species boreal forest using three scales of aerial color photos (Bolduc et al. 1999). Utilizing 3 x 3 and 5 x 5 pixel size windows, individual trees were better distinguished in the 1:10,000 photos than in the 1:5,000 or 1:20,000 photos. The authors suggested that the 1:5,000 photos were more difficult to interpret because more than one pixel could have the highest reflectance in a tree and because greater light diffusion at a higher spatial resolution could cause problems identifying tree apices (Bolduc et al. 1999).

The valley following method singles out individual trees by following and outlining the digital minima (valleys) on high spatial resolution imagery that correspond to shadows found between tree crowns. The first step of Gougeon's (1995b) automatic method for delineating tree crowns is to outline the dark pixel valleys, partially separating the background vegetation from the tree crowns. These initial valleys are subsequently masked out. A rule-based method is then applied that more precisely separates the trees and background vegetation. Crown boundaries are traced by moving pixel by pixel in a clock-wise direction around remaining local minima until the perimeter of the crown is closed. Using MEIS-II imagery (31 cm/pixel) of a conifer plantation, automated crown counts were within 7.7% of ground counts, while crown counts by human interpreters were within 8.5% to 18.1% of ground counts (Gougeon 1995b). At lower spatial resolutions, the valley following method is not as effective in separating individual trees, being more likely to isolate tree clusters (Gougeon 1998). Problems associated with this method include difficulties distinguishing individual trees among stands of small trees, thin stands, shaded stands, and stands of variable size (Gougeon 1998). Other weaknesses include the assumption that crowns are relatively round and the difficulty obtaining high crown area accuracies, especially at off-nadir angles. However, crown contour, texture, and structural information can be obtained reliably with this method (Gougeon 1998).

The template matching method involves the creation of image patterns from 3-dimensional models. The model variables include tree shape, tree height, spatial relationships of trees within a stand, background, camera angle and light condition. The modeled image patterns are applied to automatically recognize similar patterns in remotely sensed imagery, allowing the location of individual tree crowns to be predicted. Different templates for different positions within the stand may be necessary for off-nadir imagery (Larsen 1998). A template matching procedure was used to recognize individual trees in MEIS-II (36 cm/pixel) imagery of mixedwood stands in Ontario and *CASI* (60 cm/pixel) imagery of coniferous and aspen stands in Alberta (Pollack 1998). For the Ontario scene, when the actual location of an individual tree was not of concern, the template matching error was close to that of manual interpretation (10% and 11%, respectively). For correct spatial location, however, the template matching error rate (38%) was significantly higher than manual interpretation (14%) (Pollack 1998). Using the Alberta imagery, the template matching procedure was not as successful at recognizing distinct trees; however, entire tree crowns were recognized when the method succeeded. The poorer results of discriminating individual trees with the *CASI* compared to the MEIS-II imagery was partially attributed to the lower spatial resolution of the *CASI* imagery and to the tight grouping of trees in the Alberta forest (Pollack 1998). Experimenting with size, shape and placement of the match window, the template matching approach was further evaluated using geometric-optical models of scanned aerial photos of spruce trees (15 cm/pixel) (Larsen 1998). The optimal match window resulted in 91%-98% of trees delineated by manual interpretation being recovered and a standard error for tree top position of 25 cm-30 cm (Larsen 1998).

The edge contour at multiple scale method for estimating tree crown extent was tested using scanned aerial color infrared photographs (10 cm/pixel) of pure and mixed stands (pine, spruce, birch and aspen) in Sweden (Brandtberg and Walter 1998). The image first was smoothed to round off contour corners and to merge nearby parts of contours using a predetermined effective scale. Using a number of algorithms based on geometric relationships, contour edges were identified and a primal sketch of crowns was produced. From this primal sketch, seed points were established for growing tree crown segments. Compared to human interpretation, this method ignored a number of small tree crowns, but captured some tree crowns that were missed by visual interpretation. Although one to one correspondence was 66.5%, the edge contour at multiple scale algorithm resulted in almost equivalent tree crown delineation overall, as did manual interpretation (Brandtberg and Walter 1998).

Crown Closure

Textures derived from semivariogram measures taken in three directions using MEIS-II high resolution airborne imagery were used to establish limits of forest stands (St. Onge and Cavayas 1997). Stepwise regression determined the relationship between semivariogram ranges and crown diameter, stand density and crown closure, yielding R^2 values of 0.93, 0.86 and 0.89 respectively. A region growing algorithm was applied to the imagery based on stepwise regression equations in order to delineate stand boundaries (St. Onge and Cavayas 1997).

Spatial feature extraction techniques and a hierarchical per-pixel approach were compared with ground estimates for stand delineation, species composition and crown closure estimates (Gerylo et al. 1998). Using high resolution digital CCD (charged couple device) imagery (32 cm x 25 cm pixel size) of pine, spruce and aspen dominated forests in Alberta, stand estimates from the field more closely matched those using the spatial feature extraction methods than using the per-pixel method (Gerylo et al. 1998).

Leaf Area Index (LAI)

Leaf Area Index (LAI) is a measure of the area of leaf per unit area of ground, which is a measure of vegetative biomass. Along with other variables such as cover type, climate, soils, and topography, LAI inputs into ecosystem models of net primary productivity (NPP) such as BIOME-BGC (Running and Hunt 1993). Monitoring the actual NPP as a forest biodiversity element permits subtle changes in forest health or successional stage to be detected and evaluated.

Direct measures of LAI are time consuming and require destructive sampling. Using remotely sensed data, LAI has been found to correlate with vegetation indices, such as NDVI when the understory does not dominate (Spanner et al. 1984; Running et al. 1986). NDVI = (near-infrared reflectance – red reflectance)/(near-infrared reflectance + red reflectance). The relationship between LAI and NDVI is not simple, depending on species, leaf morphology, tree structure, plant health, and other factors. Values of NDVI range between –1 and +1, higher values indicate greater amounts of vegetation when other contributing factors are held constant. Also correlated with LAI, the red edge reflection point (REP) is the point of maximum slope between the boundary of chlorophyll absorption in the red wavelengths and the within leaf scattering in the near-infrared wavelengths (Lucas et al. 2000). The relationship between LAI and NDVI or REP is dependent, however, on forest structure and species. For example, regression coefficients between field measured LAI and TM-derived NDVI were 0.93 for softwood plots, 0.13 for hardwood plots and 0.66 for mixedwood plots in the Fundy Model Forest of New Brunswick (Franklin et al. 1997).

Besides leaf area index, vegetation biomass, productivity, photosynthetic activity and chlorophyll content can be estimated from the reflectance of the red edge. Models using *CASI* data (60 cm pixel) of Douglas fir stands were built that effectively distinguished areas with high and low LAI, volume and other indicators of biomass (Magnussen and Boudewyn 1998).

Forest Volume

Forest volume is the amount of wood within the forest, a more useful measure to foresters when estimated per stand rather than in larger units. Stand volume is related to stems/ha and tree diameter, which is related to tree height. Aerial photo interpretation has been used traditionally to estimate tree size directly or to estimate heights and tree proximity. Due to cost and time considerations of photo interpretation, automated approaches to forest volume estimation are welcome contributions that benefit stand level biodiversity monitoring efforts.

Expanding on the work of Eldridge and Edwards (1993), Bolduc et. al (1999) combined ancillary information with stand density estimates obtained from MEIS-II (40 cm/pixel) images in order to estimate volume of a mixed hardwood-softwood forest in Quebec. In addition to using a 3 x 3 window to identify individual trees (Eldridge and Edwards 1993), the local maxima filter was applied using a 5 x 5 window. A 5 x 5 window was used to reduce the chance of a single tree being identified as more than one by having multiple maximally bright pixels. Using this method, a map of the number of trees/ha.was achieved. Maps of tree height were also obtained in two manners: 1) as photo-interpreted height classes and 2) as heights derived from ground data. Using regression analysis, the relationship between volume and tree height was established. Then, regression analysis was employed to establish the relationship between tree height, stand density and volume. 82% of the variation in volume could be attributed to the stand density as measured by local maximally bright pixels. Including tree height, as well as stand density, 86% of the stand volume was explained (Bolduc et. al 1999).

Vegetation Stress

The absorption efficiency of chlorophyll decreases in stressed vegetation (increasing red reflectance), while the infrared reflectance decreases due to changes in the cell structure of the leaf. In stressed vegetation, change in near-infrared reflectance of leaves is often detectable before changes in the visible spectrum become apparent. Remote sensing is a useful tool for detecting vegetation stress caused by conditions as varied as disease, insect damage and drought.

Chlorosis, a visual yellowing of the leaf, occurs as the concentration of chlorophyll decreases, leaving yellow pigments to predominate in reflectance. The YI (yellowness index) quantifies leaf yellowness as the "center divided difference finite approximation of the second derivative of the reflectance spectrum" (Adams et al. 1999).

The intensity and extent of fungal tomentosus root rot (*Inonotus tomentosus*) symptoms within a spruce forest near Prince George, British Columbia was determined using *CASI* imagery (60 cm/pixel) (Reich and Price 1998). Conifer pixels were identified in the imagery by their green spectrum reflectance properties. Using the valley following approach of Gougeon (1995b), individual tree crowns were isolated. The red and near-infrared spectral characteristics of the individual tree crowns were categorized into four health classes. Using the average spectral signature of pixels within a tree crown, maximum likelihood classification successfully detected stress at the level of individual trees (Reich and Price 1998). High resolution *CASI* imagery (60 cm/pixel) was also used to assess tree infection by the fungal root pathogen *Phellinus weirii* (Laminated root rot) on the east coast of Vancouver Island, British Columbia (Leckie et al. 1998). Reduced growth, needle chlorosis, needle loss, smallish cones and mortality are symptoms of this disease. Using similar methods as Reich and Price (1998) above, mean values of pixels from individually isolated tree crowns were calculated and corrected to the mean value at nadir. Mean values for each band and several band ratios were plotted against field measures of needle loss and crown health class. Using a selected set of bands and band ratios, a classification accuracy of 77% overall by individual tree and 88% by class average resulted for the crown health classes. Moderate and severe symptoms had good detection, while light symptoms were more problematic. A number of trees were identified with no detectable symptoms on the ground (false positives) (Leckie et al. 1998).

Discriminate analysis and classification of high spatial resolution imagery has also been used to assess and map insect defoliation of forest trees (Ahern et al. 1991; Franklin et al. 1995a, b; Leckie et al. 1992; Yuan et al. 1991). In a western Newfoundland balsam fir (*Abies balsamea*) stand, the discrimination of severity classes of balsam woolly adelgid (*Adelges piceae*) infestation was evaluated using *CASI* panchromatic (25 cm/pixel) and multispectral (0.5 m and 1.0 m/pixel) imagery (Franklin et al. 1995a). From a 200 m x 100 m sample plot, 159 of 420 trees were ranked into balsam woolly adelgid damage classes, using damage class schemes of 3, 6 and 7. Based on discriminate analysis of the multispectral image bands and texture derivatives, a 40% -70% accuracy was revealed in discriminating adelgid damage classes, depending on the number of damage classes and remote sensing variables. The highest percent accuracy of class discrimination occurred using the fewest number of classes and a single pixel per tree extraction method of six spectral bands (Franklin et al. 1995a). Linear discriminate analysis tested the capability of aerial videographic data (1 m and 2 m/pixel) to separate defoliation levels, caused by western spruce budworm (*Choristoneura occidentalis*) in a mixed conifer subalpine forest in western Oregon (Franklin et al. 1995b). A strong relationship between leaf area estimates derived from field-based PAR readings and field-based percent defoliation estimates resulted from multiple regression analysis ($R^2 = 0.839$). However, multiple regression analysis showed little and weak relationships between the field estimates of percentage defoliation and the 1 m/pixel ($R^2 = 0.150$) and 2 m/pixel ($R^2 = 0.339$) imagery. The discrimination of defoliation classes for the 1 m/pixel videography was 68% accurate and 60% accurate for the 2 m/pixel imagery, improving to 78% and 68% accuracy respectively by including texture derivatives (Franklin et al. 1995b).

Change Detection

For detecting change with multi-date high spatial resolution imagery, similar problems as those associated with low spatial resolution imagery must be addressed. These include project definition, development of product specifications, data requirement analysis, determination of data availability, calculation of data acquisition costs, and data analysis cost estimates (Lunetta 1999). Normalizing for geometric, temporal, and atmospheric consistency among images is particularly important for high spatial resolution data, as small shifts in location, time or environmental conditions can cause a false detection of change.

The authors are not aware of change detection methods designed specifically for high-resolution data. Post classification comparison, classification of combined multi-date data sets, image algebra, and change vector analysis are appropriate methods for change detection for remotely sensed digital data of any resolution. Chen et al. (1999) analyzed derivative-based green vegetation index (DGVI) values from two seasons of AVRIS images in an arid region of California using image subtraction. Differences among herbaceous and shrub species in the amount of change between seasons were quantified (Chen et al. 1999). Although change detection methods are similar to those of low spatial resolution data, high spatial resolution data may differ in the purpose, areal extent, and frequency of monitoring change. High spatial resolution data may be more appropriate for detecting subtle changes in physiological processes, rather than coarser scale landscape fragmentation and human disturbance. Graphs denoting measures of processes over time may be useful for presenting these types of change, rather than representation in map form or as charts of landscape metrics.

AFBMP Pilot Study Examples

The purpose of the study examples is to illustrate the types of biodiversity elements that can be extracted from medium and high-resolution imagery.

Study Areas

The AFBMP's pilot study areas represent two of the natural regions of Alberta that are heavily forested: the Foothills and Boreal Natural Regions. In addition, the Kananaskis study area represents another more southerly, forested region of Alberta (Figure 9.1).

Foothills Pilot Area

The Foothills Pilot Area is located just south of Hinton, Alberta, centered near 53^0 15' N, 117^0 30' E (Figure 9.1). At the eastern edge of the Rocky Mountains, the landscape of this pilot area is part of the Upper Foothills Sub-Region of Alberta. The dominant forests of the sub-region are coniferous, composed of black spruce (*Picea mariana*), white spruce (*Picea glauca*), subalpine fir (*Abies lasiocarpa*) and lodgepole pine (*Pinus contorta*) stands. Deciduous trees include balsam poplar (*Populus balsamifera*), aspen poplar (*Populus tremuloides*) and willow (*Salix* spp.).

Boreal Pilot Area

The Boreal Pilot Area is located approximately 35 km west and 15 km north of Lac La Biche, Alberta, centered near 54^0 50' N, 111^0 25' E (Figure 9.1). The vegetation, climatic and soil conditions of this pilot area are characteristic of the Central Mixedwood Sub-Region of Alberta. The surface features are generally flat to modulating with low relief. Aspen poplar (*Populus tremuloides*), balsam poplar (*Populus balsamifera*) and white birch (*Betula papyrifera*) are succeeded by white spruce (*Picea glauca*) and balsam fir (*Abies balsamea*). Frequent fires play a major role in the region, eliminating older conifer stands.

Figure 9.1 Study Site Locations

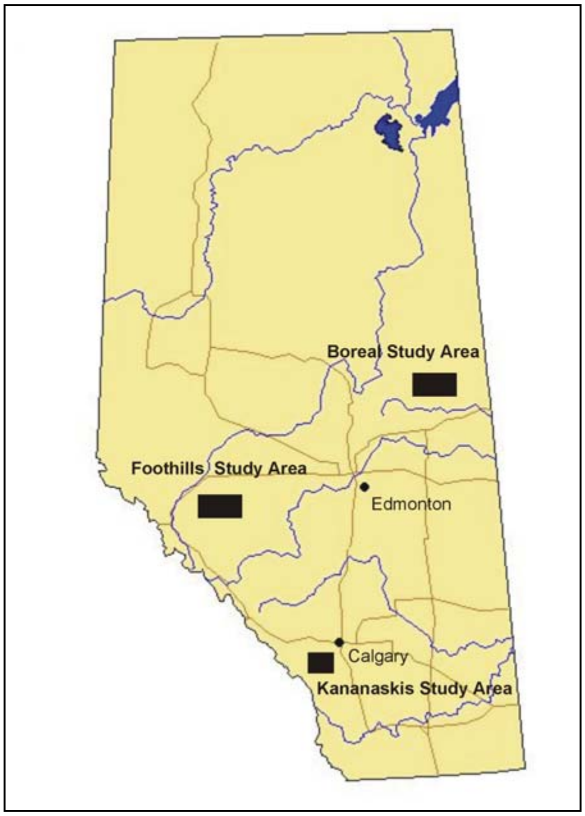

Kananaskis Study Area

The Kananaskis Study Area is located within the Kananaskis Valley to the west of Calgary, Alberta. Within a transition zone from mountain to foothills, the vegetation is characteristic of the Sub-alpine and Upper Foothills Sub-Regions of Alberta. Major tree species include lodgepole pine (*Pinus contorta*), white spruce (*Picea glauca*), Douglas fir (*Pseudotsuga menziesii*) and aspen poplar (*Populus tremuloides*). Understory contains beaked willow (*Salix bebbiana*), bearberry (*Arctostaphylos rubra*), creeping juniper (*Juniperus communis*), and wild rose (*Rosa acicularis*).

Data

Imagery

Foothills – High spatial resolution imagery was acquired on 4 August 1999 between 15:15 and 16:30 GMT using the commercial CASI. The mission was flown by Itres Research Ltd. in two straight flight lines (32 km and 31 km in length) designed to capture images from the three pilot sites (LPY, LPM, and MIX) and several National Forest Inventory (NFI) points. The first pass at an altitude of about 9,000 feet ASL captured 2 m/pixel imagery and the second pass at about 5,600 feet captured 60 cm/pixel imagery. The spectral resolutions for the imagery are given in Table 9.2. Bands were selected so as to simulate the band widths of satellite Landsat TM and to match previous CASI imagery collected in the Kananaskis region (see below). The sensor caught a continuous stream of imagery above the flight lines, 63 km in total, providing ample data for future analyses.

Boreal – Immediately after completing the Foothills mission, the Beechcraft B80 QueenAir aircraft operated by Itres Research Ltd. flew northeast to the Boreal Study Area. In a similar fashion, two straight flight lines were designed to collect 2 m (at about 7,100 feet ASL) and 60 cm (3,600 feet ASL) imagery of three pilot sites (CON, DEC, MUS) (Figure 9.3) as well as NFI points. The CASI imagery of the Boreal area was obtained approximately between 20:35 and 22:00 GMT on 4 August 1999. The total length of imagery of the Boreal study area is 73 km (30 + 43).

Table 9.2 Spectral Resolution Casi Data – Foothills and Boreal Study Areas

60 cm CASI		2 m CASI			
Band	Wavelength (nm)	Band	Wavelength (nm)	Band	Wavelength (nm)
1	449.4 to 500.2	1	427.1 to 449.8	10	714.0 to 729.6
2	539.3 to 560.3	2	449.4 to 498.3	11	729.3 to 754.5
3	609.2 to 639.9	3	498.0 to 519.0	12	754.2 to 789.1
4	639.6 to 679.9	4	518.6 to 539.6	13	788.8 to 810.3
5	689.1 to 716.2	5	539.3 to 558.5	14	810.0 to 829.6
6	729.3 to 754.5	6	558.1 to 590.6	15	829.3 to 850.8
7	790.7 to 810.3	7	609.2 to 639.9	16	850.5 to 857.9
		8	639.6 to 679.9	17	875.7 to 889.5
		9	689.1 to 714.2	18	900.9 to 959.4

Itres Research Ltd. provided digital data with standard radiometric calibration and georeferencing in 1.6 Gb or smaller files in exabyte format. The imagery was transferred from exabyte format to PC format using facilities in the Faculty of Environmental Design, University of Calgary before storing as .pix files (PCI file format) on standard CDs.

Figure 9.2 CASI Imagery (2m and 60 cm) with Field Measures - AFBMP Foothills Pilot Sites

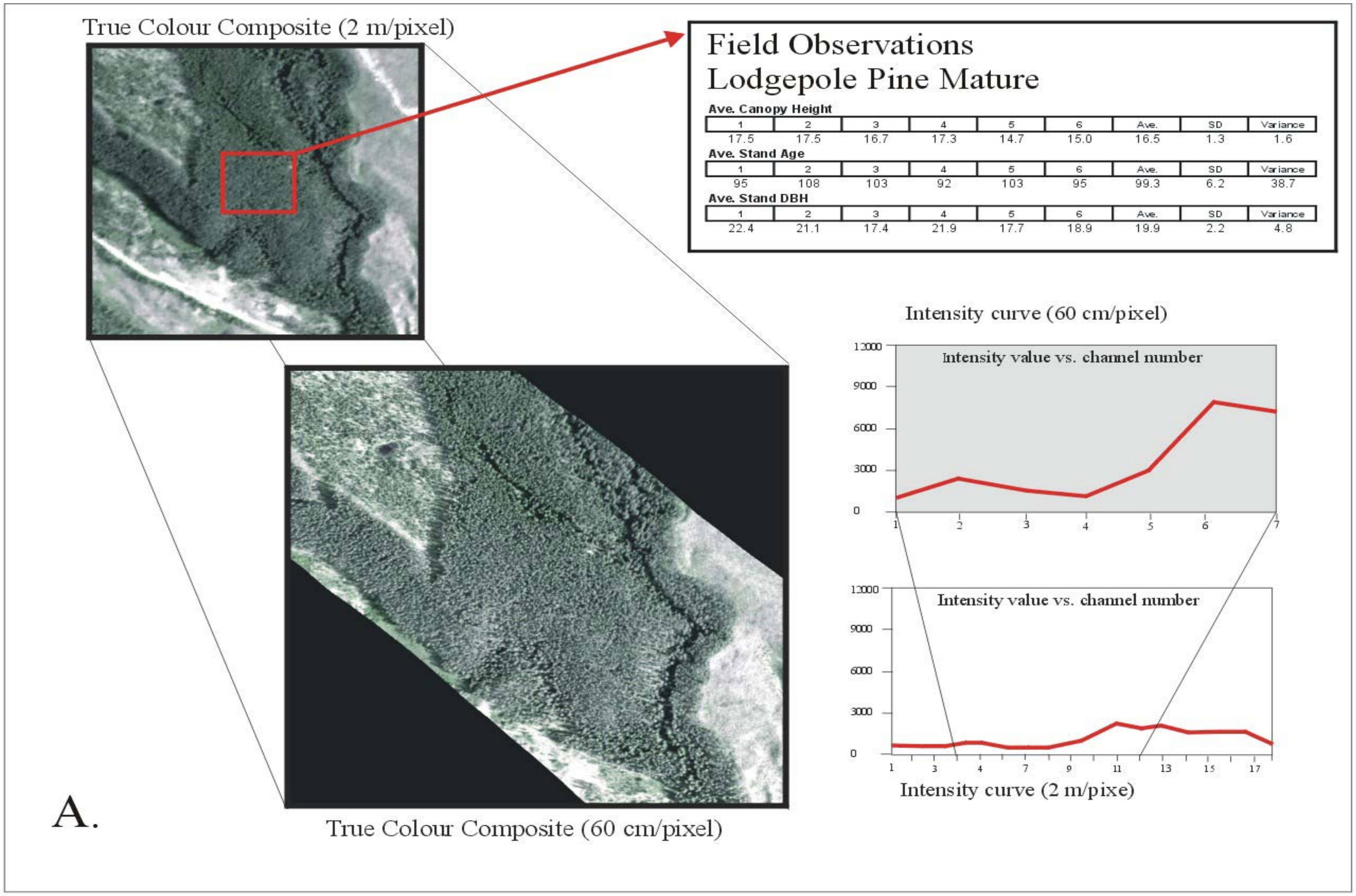

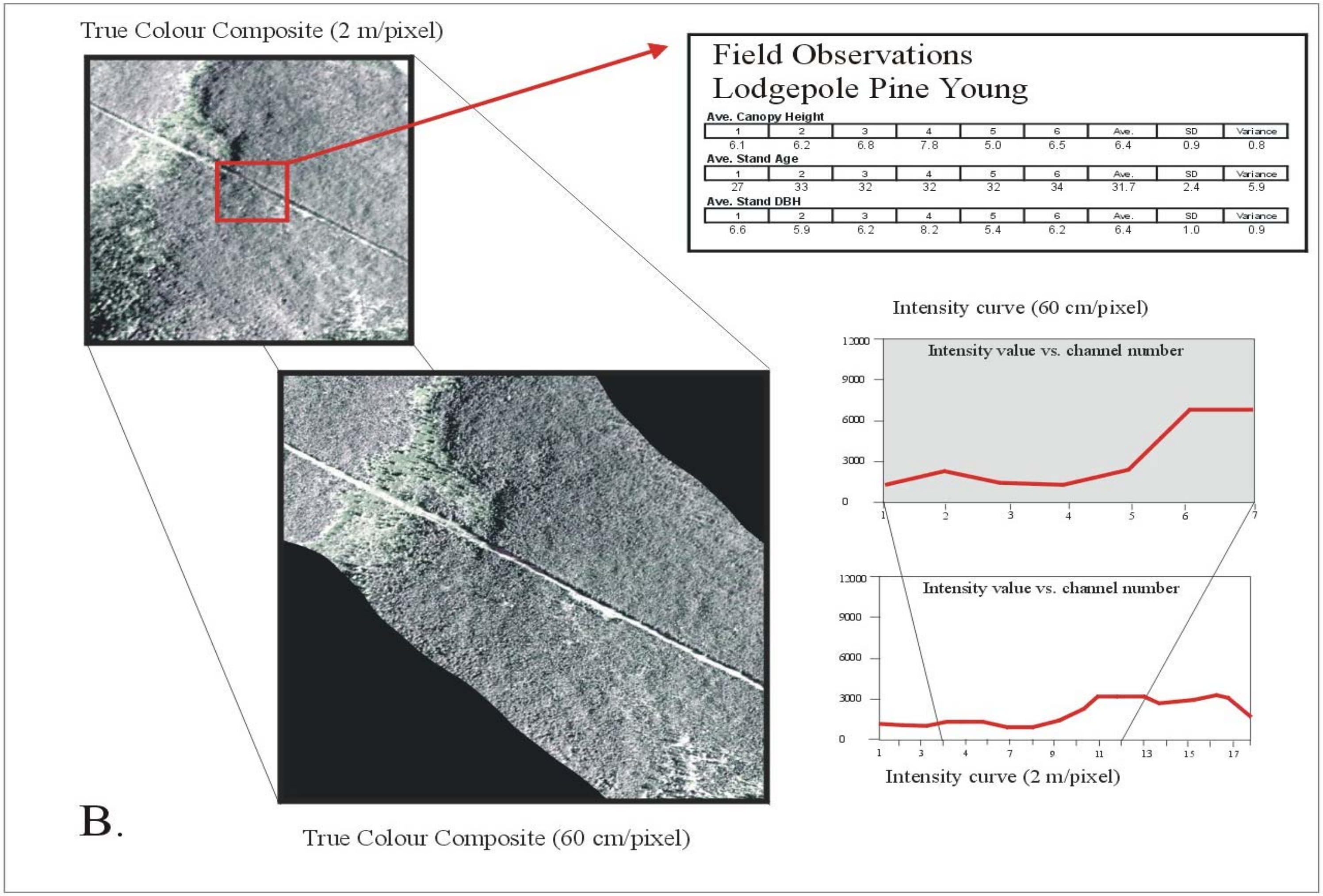

Ave. Canopy Height

1	2	3	4	5	6	Ave.	SD	Variance
6.1	6.2	6.8	7.8	5.0	6.5	6.4	0.9	0.8

Ave. Stand Age

1	2	3	4	5	6	Ave.	SD	Variance
27	33	32	32	32	34	31.7	2.4	5.9

Ave. Stand DBH

1	2	3	4	5	6	Ave.	SD	Variance
6.6	5.9	6.2	8.2	5.4	6.2	6.4	1.0	0.9

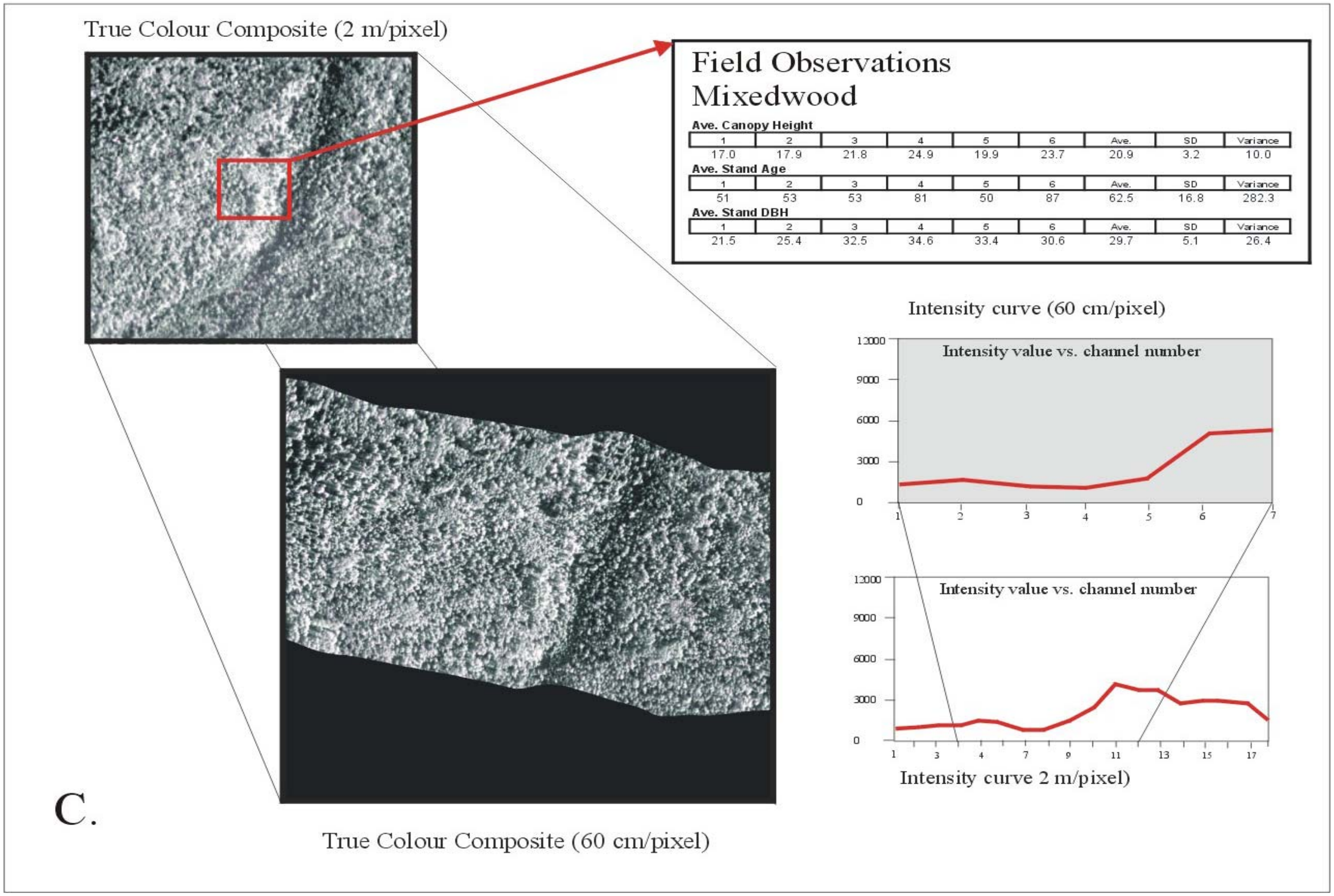
True Colour Composite (2 m/pixel)
Field Observations
Mixedwood
Ave. Canopy Height
1 2 3 4 5 6 Ave. SD Variance
17.0 17.9 21.8 24.9 19.9 23.7 20.9 3.2 10.0
Ave. Stand Age
1 2 3 4 5 6 Ave. SD Variance
51 53 53 81 50 87 62.5 16.8 282.3
Ave. Stand DBH
1 2 3 4 5 6 Ave. SD Variance
21.5 25.4 32.5 34.6 33.4 30.6 29.7 5.1 26.4
Intensity curve (60 cm/pixel)
Intensity value vs. channel number
Intensity value vs. channel number
Intensity curve 2 m/pixel)
C.
True Colour Composite (60 cm/pixel)

Figure 9.3 CASI Imagery (2m and 60 cm) with Field Measures - AFBMP Boreal Pilot

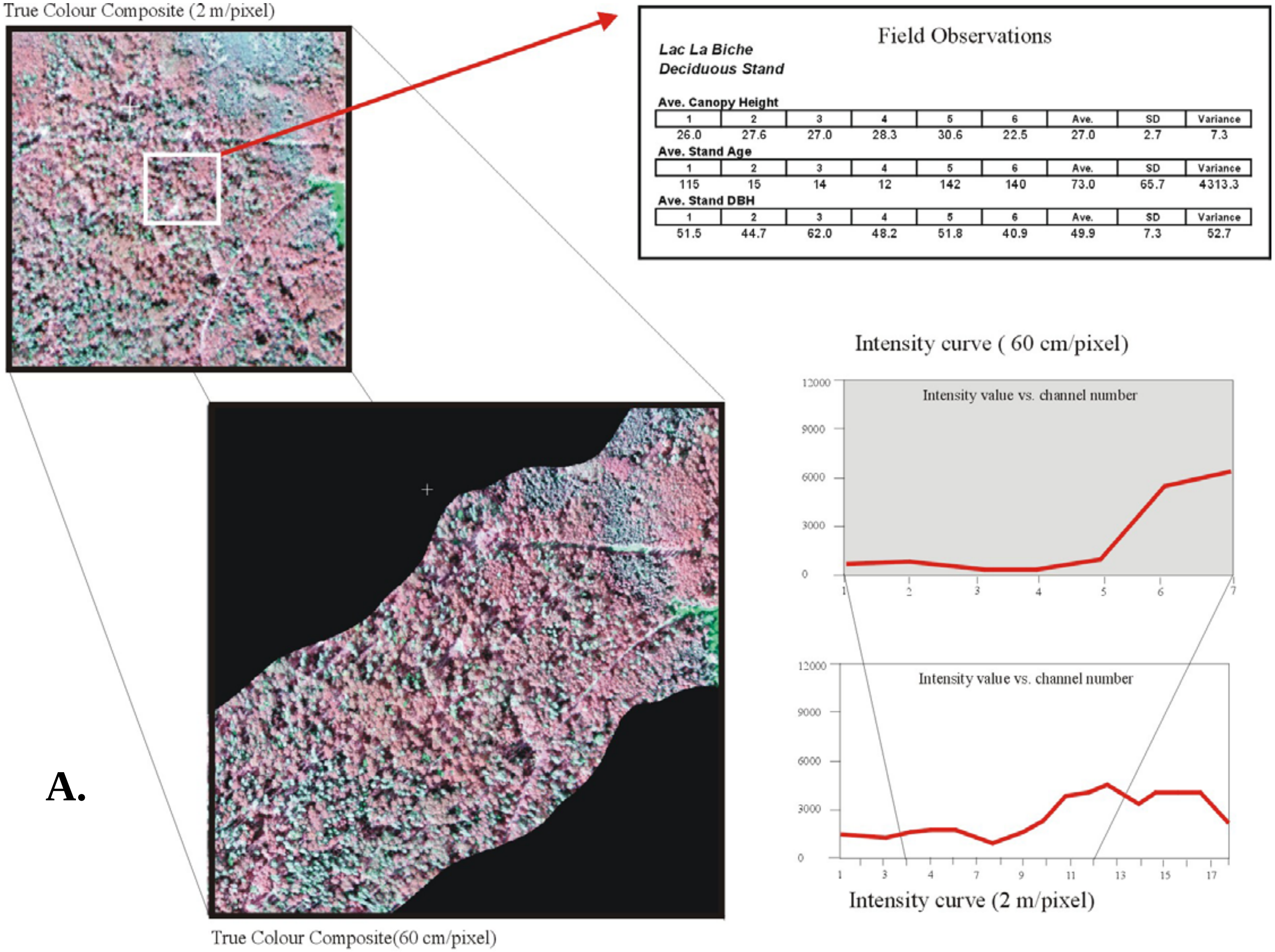

Field Observations

Lac La Biche
Deciduous Stand

Ave. Canopy Height

1	2	3	4	5	6	Ave.	SD	Variance
26.0	27.6	27.0	28.3	30.6	22.5	27.0	2.7	7.3

Ave. Stand Age

1	2	3	4	5	6	Ave.	SD	Variance
115	15	14	12	142	140	73.0	65.7	4313.3

Ave. Stand DBH

1	2	3	4	5	6	Ave.	SD	Variance
51.5	44.7	62.0	48.2	51.8	40.9	49.9	7.3	52.7

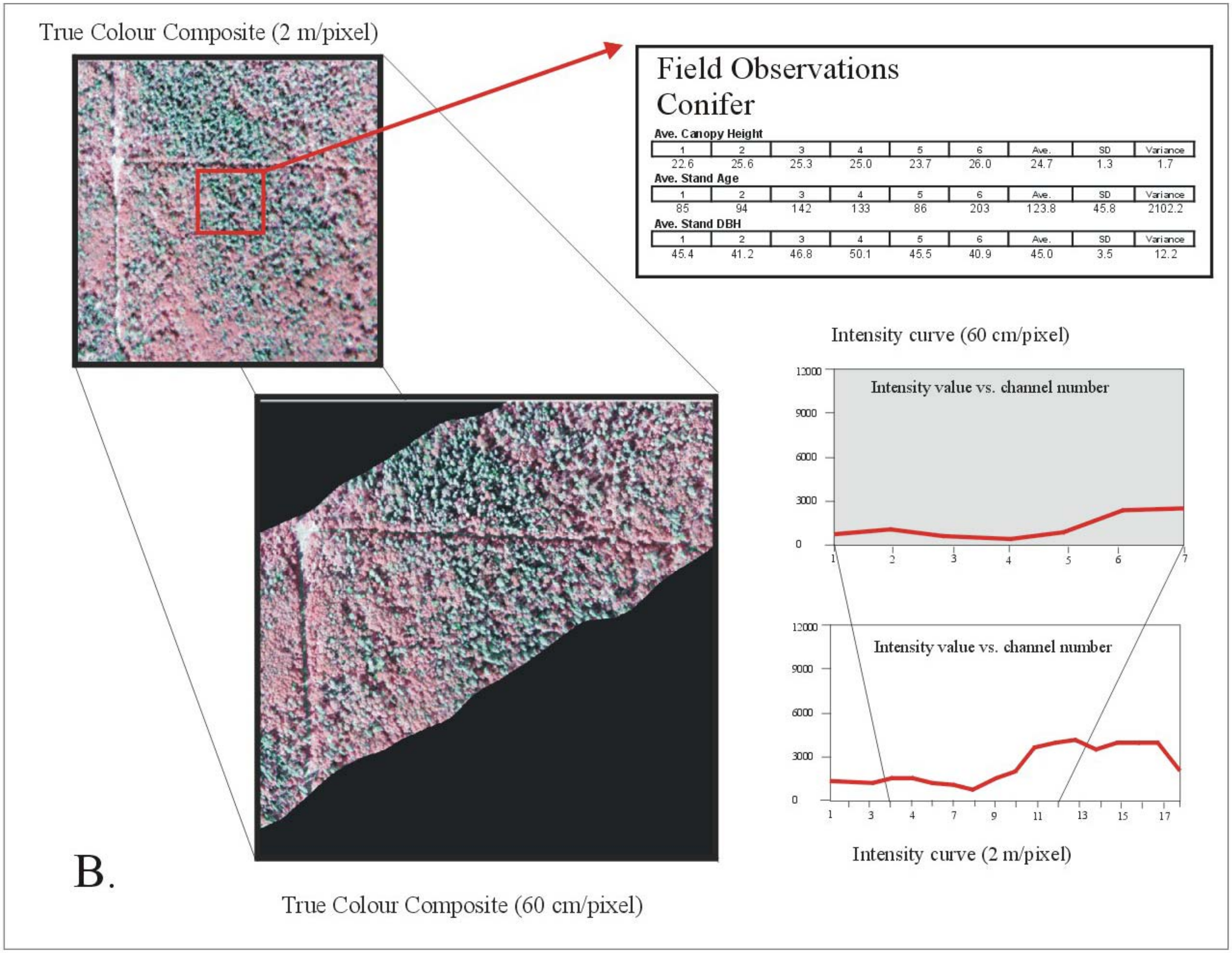

Ave. Canopy Height

1	2	3	4	5	6	Ave.	SD	Variance
22.6	25.6	25.3	25.0	23.7	26.0	24.7	1.3	1.7

Ave. Stand Age

1	2	3	4	5	6	Ave.	SD	Variance
85	94	142	133	86	203	123.8	45.8	2102.2

Ave. Stand DBH

1	2	3	4	5	6	Ave.	SD	Variance
45.4	41.2	46.8	50.1	45.5	40.9	45.0	3.5	12.2

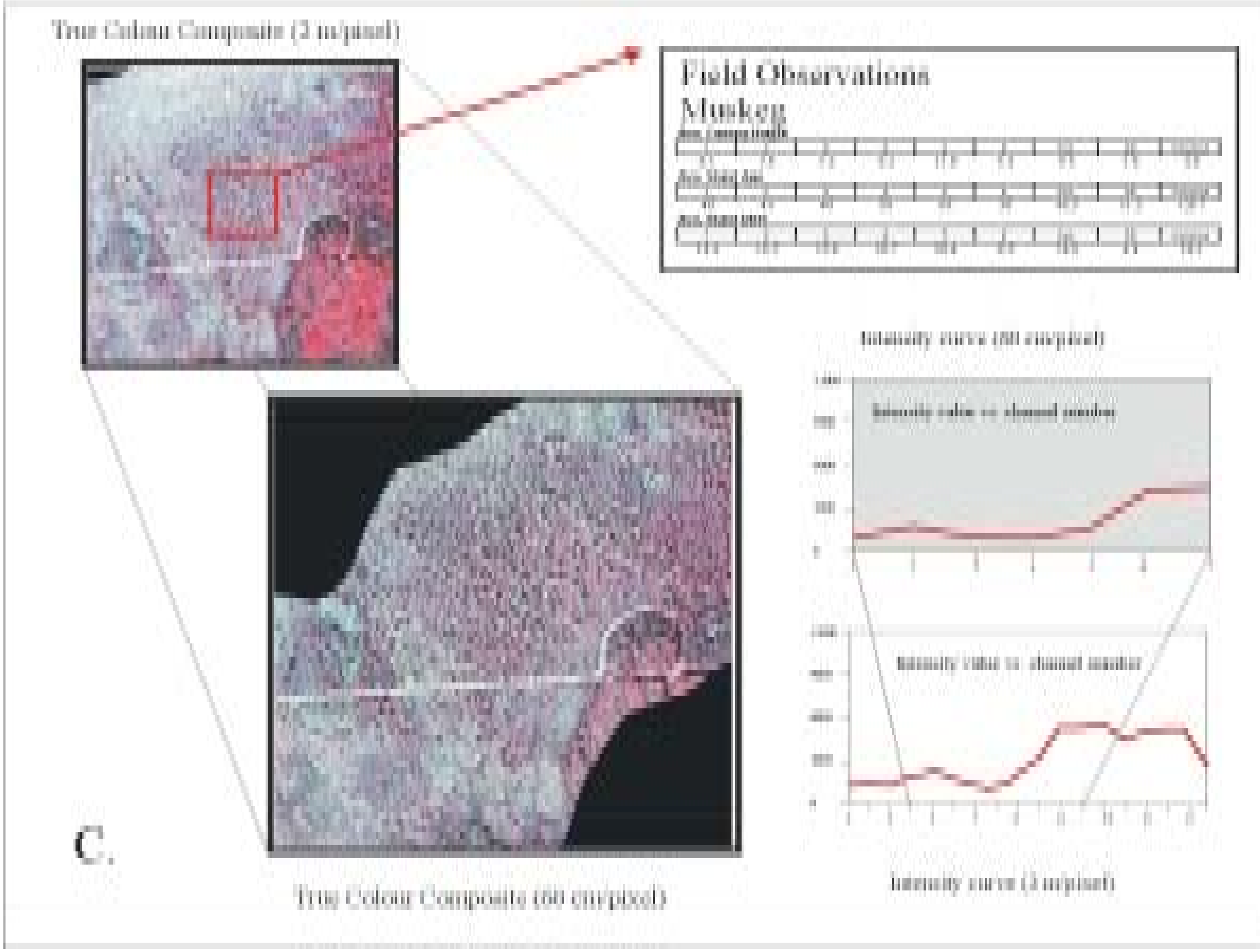
True Colour Composite (2 m/pixel)
Field Observations
Muskeg
Intensity curve (60 cm/pixel)
Intensity value vs channel number
Intensity value vs channel number
Intensity curve (2 m/pixel)
C.
True Colour Composite (60 cm/pixel)

Different spectral characteristics are captured at different spatial resolutions. At higher spatial resolutions, the sensor is able to record fewer spectral bands than at lower spatial resolutions. By collecting both 60 cm and 2 m spatial resolution data, the greater spatial detail of the 60 cm data is enhanced with the greater spectral detail of the 2 m data. By having both types of data, classifications can be improved.

In order to measure spectral intensity from images of areas nearly equal size on the ground, an 11 x 11 pixel window was sampled for the 60 cm and a 3 x 3 pixel window for the 2 m data. Figures 2 and 3 illustrate spectral intensity curves for 60 cm and 2 m data taken from each AFBMP pilot site. As can be seen in these figures, the total bandwidth of the 2 m imagery is greater than for the 60 cm (Table 9.2). In the case of the Foothills pilot site, the intensity curves are higher for the 60 cm than for the 2 m data (Figure 9.2), while for the Boreal pilot sites the curves are lower for the 60 cm data (Figure 9.3). However, greater spectral detail is reflected in the higher variability of the 2 m intensity curves because there are more bands.

Kananaskis – Itres Research Ltd. Conducted a CASI mission that captured imagery over the study area on 18 July 1998 between 11 AM and 2 PM (Figure 9.1). The timing of the mission was planned to correspond to maximum leaf-on, clear atmospheric conditions and optimum light conditions. The seven spectral bands for 60 cm data and the 18 spectral bands for 1 m and 2 m data were chosen so that they could be combined into the same band intervals as Landsat TM bands.

Field Data

Foothills – The AFBMP's vegetation pilot study group (Alberta Research Council (ARC), Vegreville) provided data for three pilot sites in the Foothills: LPY (lodgepole young); LPM (lodgepole mature); and MIX (mixedwood). Circular sample plots and transect lines were measured within each pilot site. The nested circular (6 and 10 m diam) plots were located in the center and on each of the four sides of a 100 m x 100 m plot, oriented with two sides facing north. Transects of 100 m in length were laid out in a north-south direction at the center and on either side parallel and 25 m from the center transect. From the 6 m diam plots, trees less than 7 cm DBH were measured for species and DBH. From the 10 m diam plots, the same measures were taken for trees greater than 7 cm DBH. Taken along transect lines were large tree and snag data including species, dead or living condition, DBH, and decay index. In addition, six trees from each pilot site were selected to represent the dominant canopy height. For these six trees, the species, canopy height, tree age, and DBH were recorded (Figure 9.2). GPS readings were taken at the centers and corners of the 100 m x 100 m pilot plots.

Boreal – For the Boreal study area, vegetation data were collected by ARC using the same plot design and methods as used for the Foothills. The three pilot sites of the Boreal study area are CON (conifer), DEC (deciduous), and MUS (muskeg) (Figure 9.3).

Kananaskis – Using standardized methods, field measures in the Kananaskis field study area were contributed by a number of investigators and institutions (University of Calgary, University of Lethbridge, Canadian Forest Service and ARC). More complete field methods used in Kananaskis are described in Moskal (1999). 10 m x 10 m plots were sampled along transects that crossed through conifer and deciduous (pure and mixed) stands. Tree species, tree height and height to canopy, tree diameter at breast height, and crown diameter were measured for each tree within the plots. For each plot, other measures taken included slope, aspect, GPS readings, stem plots and crown closure estimates. These measurements provide the basis for determining Alberta Vegetation Inventory (AVI) labels for each plot.

Analyses

For the following examples, image enhancements and classifications were performed using the image analytic software PCI. Statistical analyses were performed using SPSS and Excel.

Example 1 - Number of Trees

Using three stand types (deciduous, coniferous, and mixed woods) taken from separate areas within the1998 Kananaskis 60 cm CASI imagery, pixels representing shadows and understory were first identified by a pixel by pixel supervised classification and then extracted (masked out) from further analysis. For the remaining pixels representing tree crowns, a local maxima technique was employed to identify brightest pixels within the crown, under the assumption that these brightest pixels represent tree apices. Locally brightest pixels are highlighted after the shadow and understory are removed (Figure 9.4). For the coniferous stand, the tree apices (locally brightest pixels) were simply counted. In this example, a count of seventy conifer apices within a 100 x 100 pixel block results (stand density = 116.7 trees/ ha) (Figure 9.4).

For the deciduous stand with broader tree canopies, the method was modified to compensate for more than one apex occurring per tree, based on estimated crown diameter. One count is tallied for all identified apices within a given area, which is determined by the average crown diameter within the stand. For this example, the decision rule was to count as one apex, all brightest pixels within a 5 x 5 pixel area (3 m x 3 m). Using this decision rule within a 33 x 33 pixel sub-image of deciduous trees, the number of apices counted is 23, or 352 trees/ha (Figure 9.4).

Two separate paths were taken for counting trees in the mixed wood sub-image. Pixels classified as conifer apices were counted directly, whereas the pixels classified as deciduous apices within a 5 x 5 pixel area were counted as one apex. In this example, pixels classified as conifer are green, while those classified as deciduous are blue (Figure 9.4). This approach results in 10 conifer and seven deciduous apices being enumerated within a 52 x 52 pixel block of the mixed wood sub-image. The stand density is 43.1 coniferous and 61.6 deciduous trees/ha (Figure 9.4).

Figure 9.4 Tree Counts from CASI Imagery (60 cm): Kananaskis Study Area

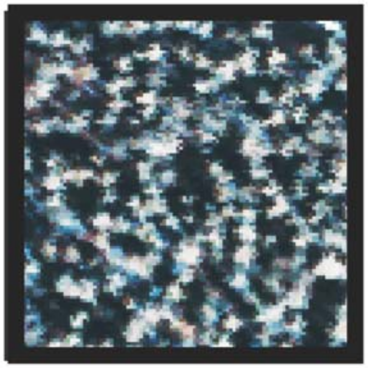

False colour image

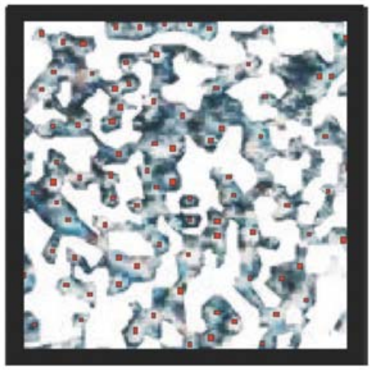

Shadow and understory removed

CONIFER STAND

70 Counts
Based on maximally bright pixels

117 trees/hectare

False colour image

Shadow and understory removed

DECIDUOUS STAND

23 Counts
Based on maximally bright pixels, only one count when within a five pixel radius

352 trees/hectare

False colour image

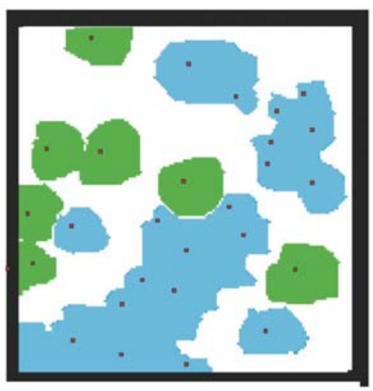

Shadow and understory removed
Species classified

MIXEDWOOD STAND

Classification followed by maximally bright pixel counts; method depends on species

Conifer - 7 counts
Deciduous - 10 counts

43 conifer trees/hectare
62 deciduous trees/hectare

Example 2 – Crown Closure

Crown closure estimates obtained from the high spatial resolution CASI imagery are compared to field estimates of crown closure in the Kananaskis study area. Field measures of crown closure were collected using a spherical crown mirror densiometer. In addition, percent crown closure from AVI determinations using classified CASI imagery are compared to those obtained in the field. AVI crown closures in the field are based on the basal area of the dominant species per canopy cover, measured in 10% units.

For one sub-scene of the1998 CASI imagery (60 cm), two approaches were used to extract crown closure estimates: 1) Laplacian filter; and 2) supervised classification. The Laplacian is a second derivative, edge enhancement filter. When the Laplacian filtered is passed over forest stand imagery, high contrast regions between tree crowns and shadows (and understory) are emphasized. Based on the brightness values of the resulting Laplacian image, pixels are separated into two classes, crown and other. The percentage of pixels in the crown class is then calculated. In the Kananaskis example, crown closure estimates based on the Laplacian filter method (61%) and classification (55%) are close to those obtained from field estimates (57%) (Figure 9.5).

Figure 9.5 Crown Closure - Laplacian Filter CASI Imagery (60 cm) - Kananaskis Study Area

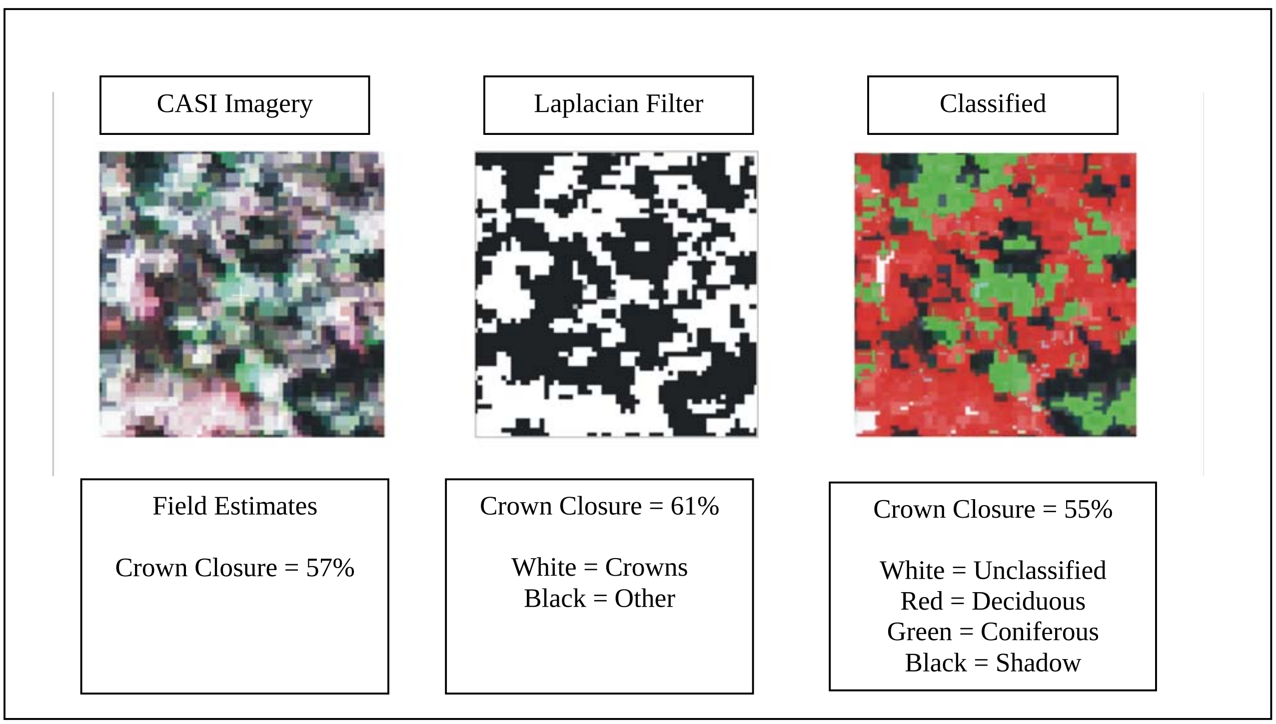

For other areas in the Kananaskis study area, crown closure estimates and AVI information extracted from classified CASI imagery are compared to those obtained in the field (Figure 9.6). Six sub-scenes were chosen for this example that vary in percent species composition. AVI abbreviations used in this example are given in Table 9.3.

Table 9.3 SELECTED AVI TREE SPECIES LABELS

Common Name	Latin Name	AVI Label
White Spruce	*Picea glauca*	Sw
Black Spruce	*Picea mariana*	Sb
Lodgepole Pine	*Pinus contorta*	Pl
Trembling Aspen	*Populus tremuloides*	Aw
Larch, Tamarack	*Larix laricina*	Lt

No more than a 10% difference in species cover occurs between the field calls of AVI and the AVI determined from classification (Figure 9.6). For example, for the plot illustrated by Figure 9.6a, the field call for AVI was Pl_{10} (100% Lodgepole Pine) and the classification for AVI was Pl_9AW_1 (90% Lodgepole Pine, 10% Trembling Aspen).

The difference between the field and classification estimates of crown closure range from 2% to 6%, with the classification estimates always higher (Figure 9.6). In Figure 9.5, for example, crown closure was estimated as 55% in the field and 61% from the classified image. One factor that may contribute to differences between the image and field estimates of both the AVI and crown closure is that the areal extent of the imagery is larger than the field plots.

Example 3 - Vegetation Stress – Aspen Defoliation

Pure and mixed aspen (*Populus tremuloides*) stands, as well as conifer, comprise the forest of the Kananaskis study area. Various levels of leaf defoliation were observed among aspen stands near Barrier Lake during the 1998 Kananaskis field season (Moskal 1999) that provide an example of natural vegetation stress in an Alberta forest. The cause of the leaf defoliation in these aspen stands was identified as Bruce spanworm (*Operophtera bruceata*). Bruce spanworm overwinters as eggs in the bark or in moss on the ground near the tree. The spanworm larvae emerge from the eggs to feed on leaf material within the bud or on early leaves expanding in the spring (Peterson and Peterson 1992). Perforated or severely reduced leaves result as larvae chew into the bud or emerging foliage. The amount of leaf biomass and levels of stress of the affected aspen are ultimately determined by the level of insect infestation. Aspen stands were identified in Kananaskis with low, moderate and high levels of aspen defoliation and their spectral curves compared. From high spatial resolution CASI imagery (60 cm/pixel), the spectral reflectance curves of defoliated aspen can be seen to differ from that of healthy aspen; defoliated trees have lower near-infrared and higher green and red reflectance than do healthy aspen (Figure 9.7). These differences are great enough to be observable in false color CASI imagery that display these aspen stands with three different levels of defoliation (Figure 9.7). These differences are partially due to the lower photosynthetic activity and water content that is found in stands with lower leaf biomass than in those with higher biomass. In addition, reflectance from the understory and non-leafy parts of the tree (stem and bark) can filter through the perforated leaves, contributing more to spectral signatures of stands with high levels of defoliation.

Figure 9.6 Crown Closure and AVI Estimates: Field and Classification - CASI Imagery (60 cm) Kananaskis Study Area

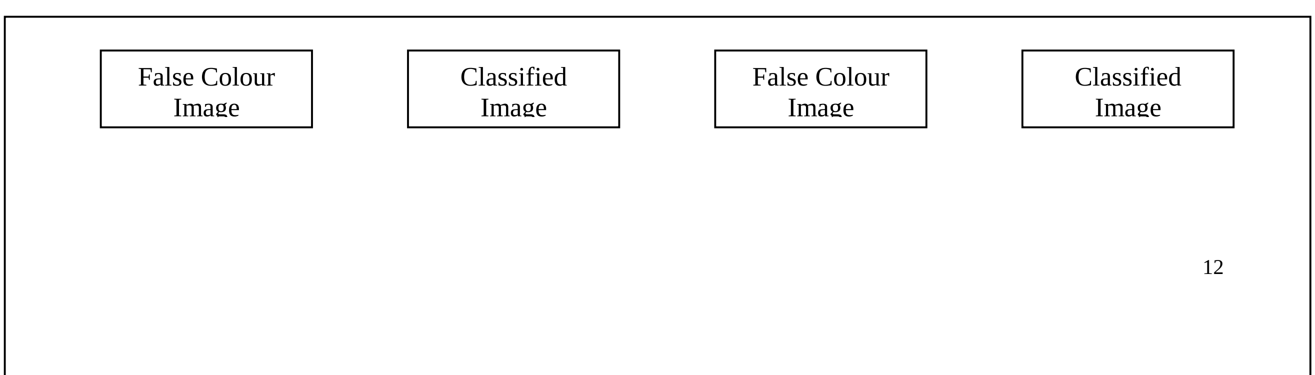

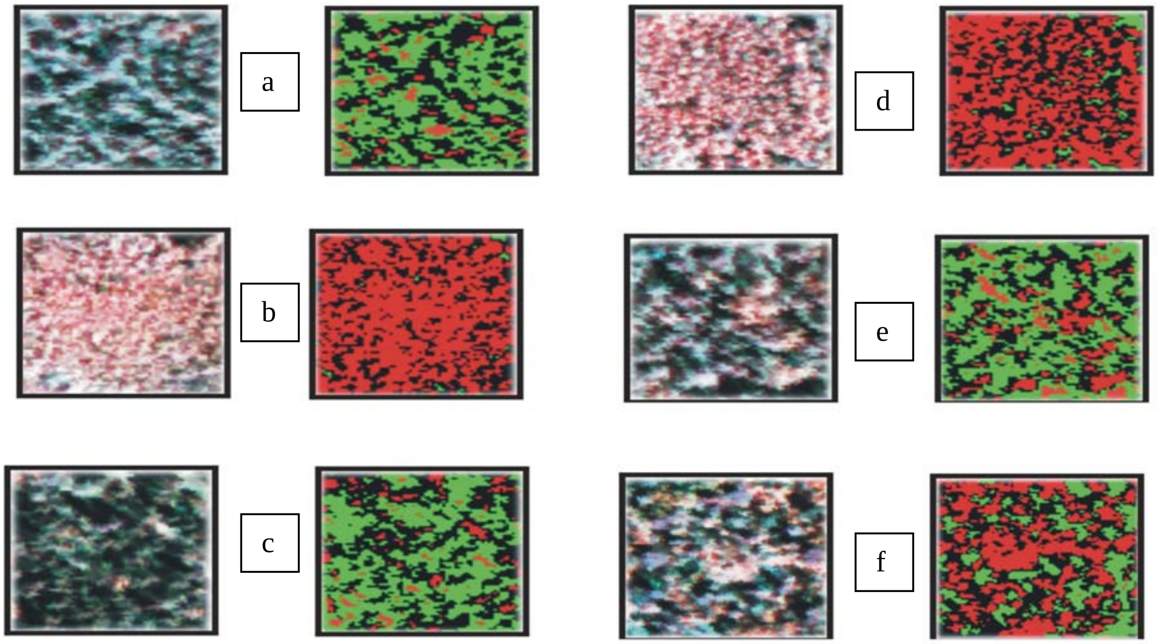

Field Estimates			Classified Image Estimates	
AVI		Crown Closure	AVI	Crown Closure
a	Pl_{10}	61%	Pl_9Aw_1	65%
b	Aw_{10}	70%	Aw_{10}	75%
c	Sw_9Aw_1	64%	Sw_9Aw_1	69%
d	Aw_9Sw_1	60%	Aw_8Sw_2	62%
e	Sw_7Aw_3	55%	Sw_8Sw_2	61%
f	Aw_5Pl_5	58%	Aw_5Pl_5	62%

Figure 9.7 Aspen Defoliation: Low, Medium, High - CASI Imagery (60 cm) Kananaskis Study Area

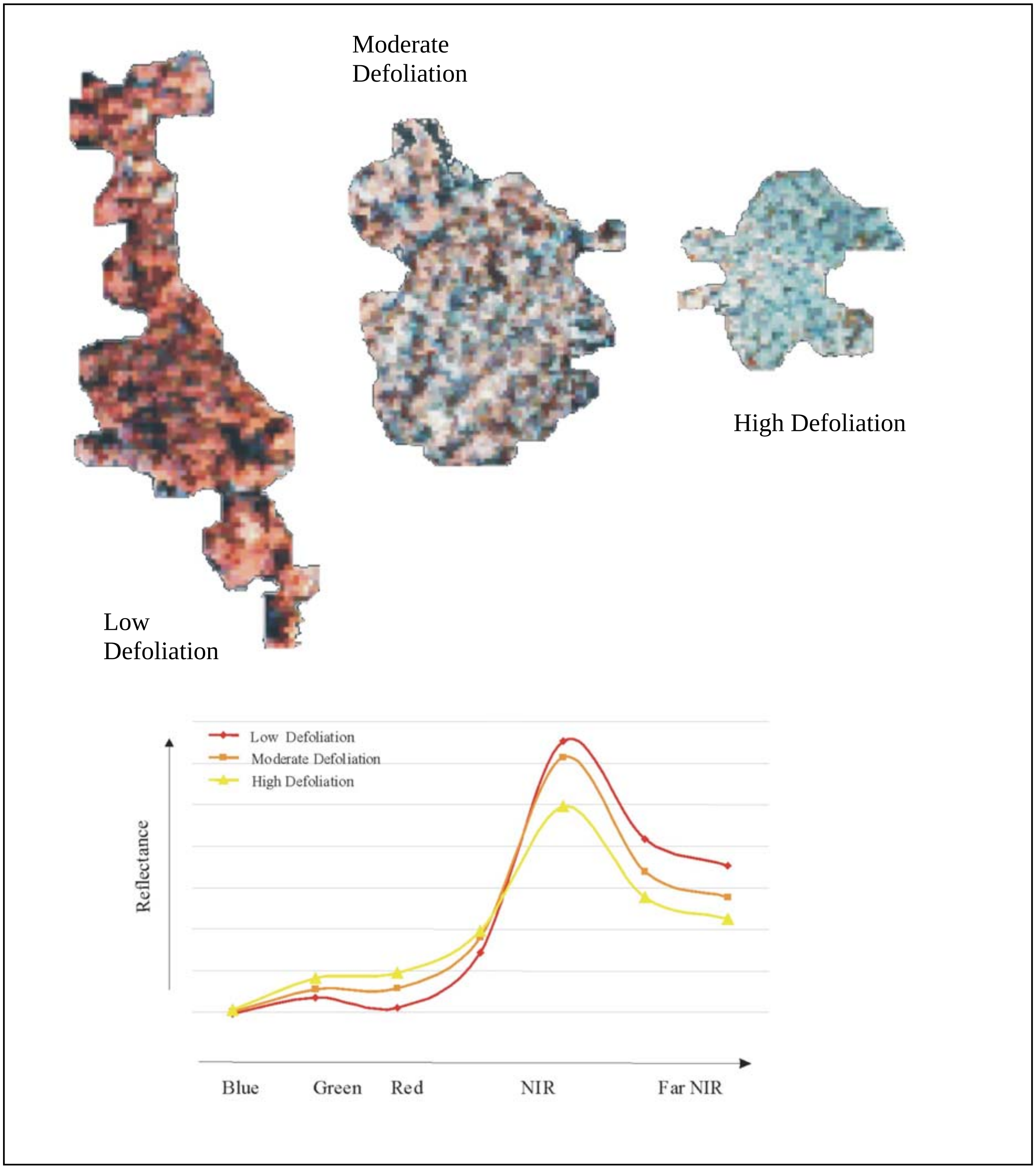

Example 4 – Canopy Roughness and Image Texture

Canopy roughness refers to the variation in vertical structure of the canopy. A stand with a large variance in tree height has a rougher upper canopy than a stand with a small variance in tree height (Figure 9.8). Young, even-aged stands of pure species tend to have smoother upper canopies than mixed-aged mixedwood stands. Larger shadows of trees are cast in stands of uneven height than in stands of even height. Furthermore, in stands of varying tree heights, the shadows are less uniform in their spatial distribution. These differences in tone and texture between smooth and rough canopy surfaces can be distinguished within medium and high spatial resolution remotely sensed imagery.

Figure 9.8 Canopy Roughness

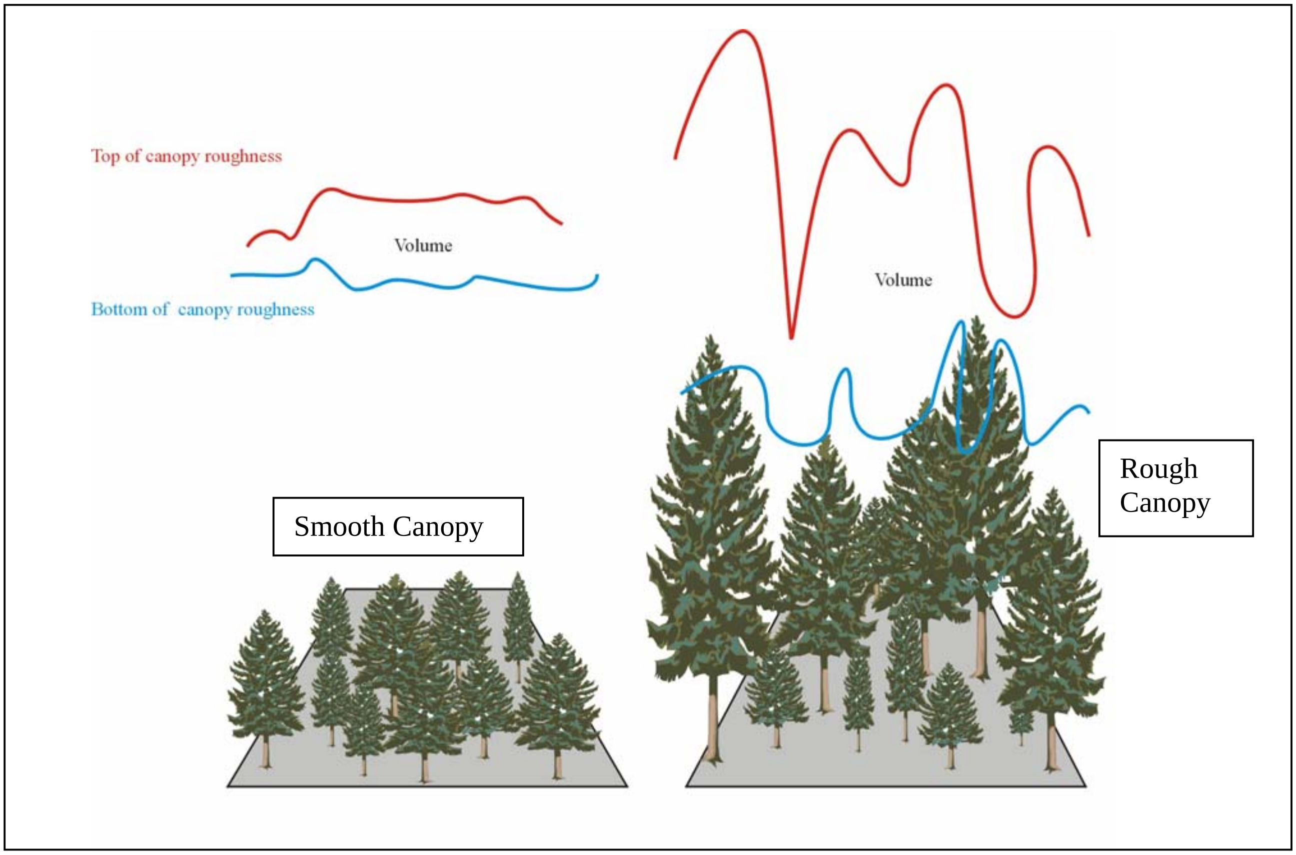

For example, tone and textural differences are visually detectable among CASI images of Lodgepole pine stands in the Foothills pilot sites LPY (young stand) and LPM (mature stand) (Figures 9.9 and 9.10). Based on measures of canopy height provided by ARC, the mature Lodgepole pine stand site is more variable (rougher canopy) than the young stand site. The estimated average canopy height for the mature Lodgepole pine stand is 16.5 m (S.D. = 1.3, Var = 1.6), and for the young stand, 6.4 m (S.D. = 0.9, Var. = 0.8). The young pine stand image (Figure 9.9) is brighter with a smaller variation in discrete tonal features than is the mature pine stand image (Figure 9.10). For the young pine stand image, more pixels representing crowns that are highly reflective create a relatively bright scene compared to the mature pine stand image, where more shadow pixels predominate. Although difficult to discern at the scale of these figures, the distribution of dark and light areas is more evenly distributed in the young pine stand image than in the mature pine stand (Figures 9.9 and 9.10).

To quantify the spatial distribution of tonal features within an image band, texture derivatives can be produced and output as images. For envisioning homogeneity, the texture values are scaled between 0 and 255; brighter areas (higher digital number values) corresponding to regions that are more uniform or unvarying than darker areas (lower digital number values). Available in PCI, the following homogeneity texture algorithm was utilized in this example.

Homogeneity = SUM (i,j=0,N-1)(P(i,j)/(1+(i-j)**2)), where N is the number of grey levels.
P is the normalized symmetric Grey Level Co-occurrence Matrix of dimension N x N.
P(i,j) is the normalized co-occurrence matrix such that SUM(i,j=0,N-1)(P(i,j)) = 1
V(k) is the normalized grey level difference vector
V(k) = SUM(i,j=0,N-1 and |i-j|=k) P(i,j)

This algorithm results in homogeneity texture values that vary between 0 and 1.

Several sized windows were moved across the 60 cm and 2 m near-infrared image bands (interval of 639.6 nm to 679.9 nm) of LPY and LPM to produce homogeneity texture derivatives for each pixel and to calculate the average homogeneity value of the image. For illustration, a 15 x 15 pixel window for the 2 m data and a 31 x 31 pixel window for the 60 cm data were selected because they gave the maximum difference in average texture values for the two pine stands (Figures 9.9 and 9.10). The average homogeneity value for the 2 m LPY image (0.42) is 10% higher than the value for the 2 m LPM image (0.32). For the 60 cm sample images, the texture values are more similar between the two stand types. However, the average homogeneity value of LPY (0.37) is still 4% higher than the value of LPM (0.33). As expected, the younger stand with more evenly sized trees has a smoother image pattern (greater homogeneity) than the older stand.

For biodiversity monitoring, changes in canopy roughness could indicate significant changes within a stand that are caused by succession, disturbance or uneven growth. In addition, there may be a direct relationship between canopy structure and biodiversity, as certain species have vegetation structural preferences and/or requirements.

Figure 9.9 Canopy Roughness and Texture - Foothills Study Site Lodgepole Pine Young (LPY)

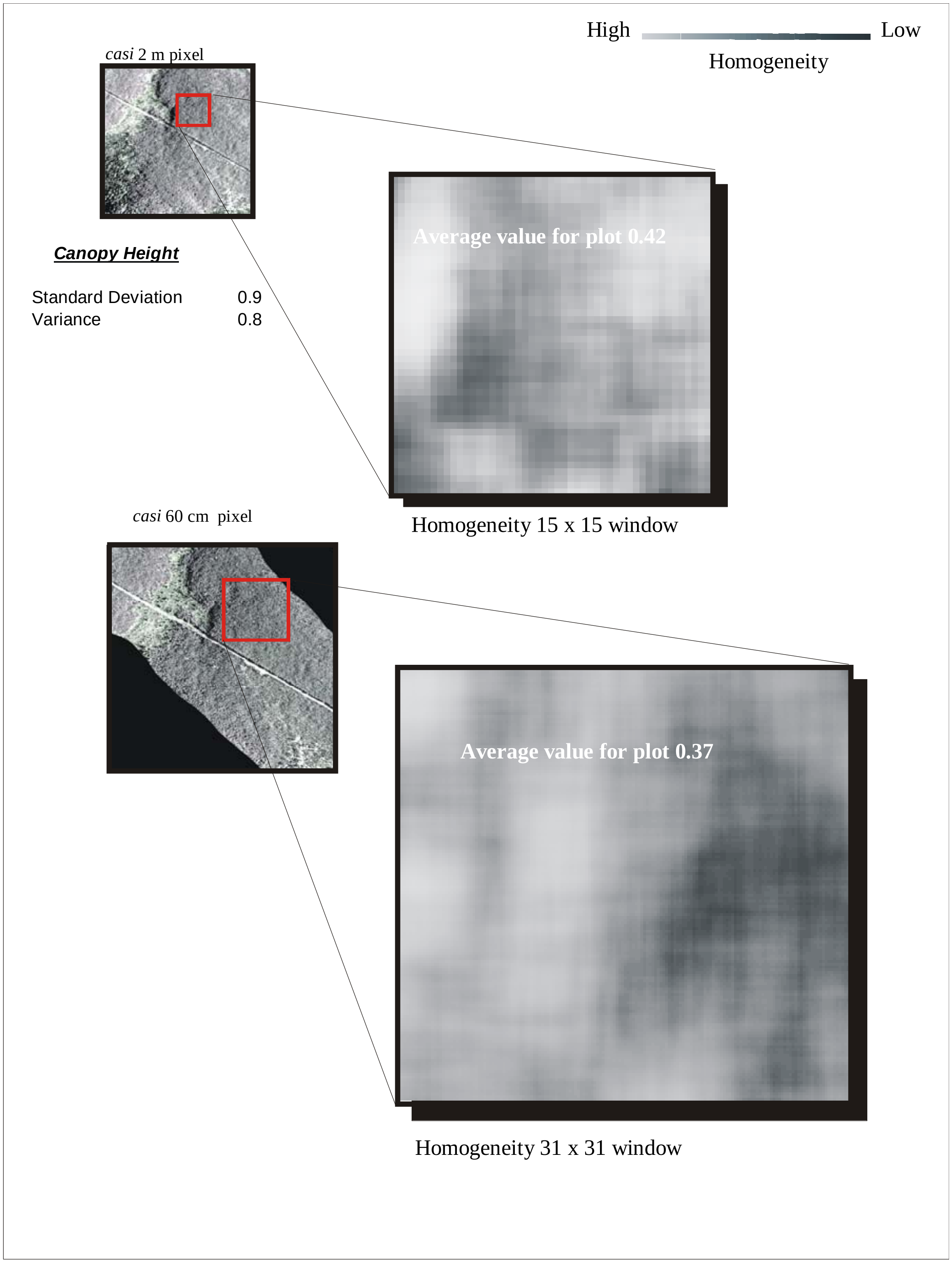

Figure 9.10 Canopy Roughness and Texture - Foothills Pilot Site, Lodgepole Pine Mature (LPM)

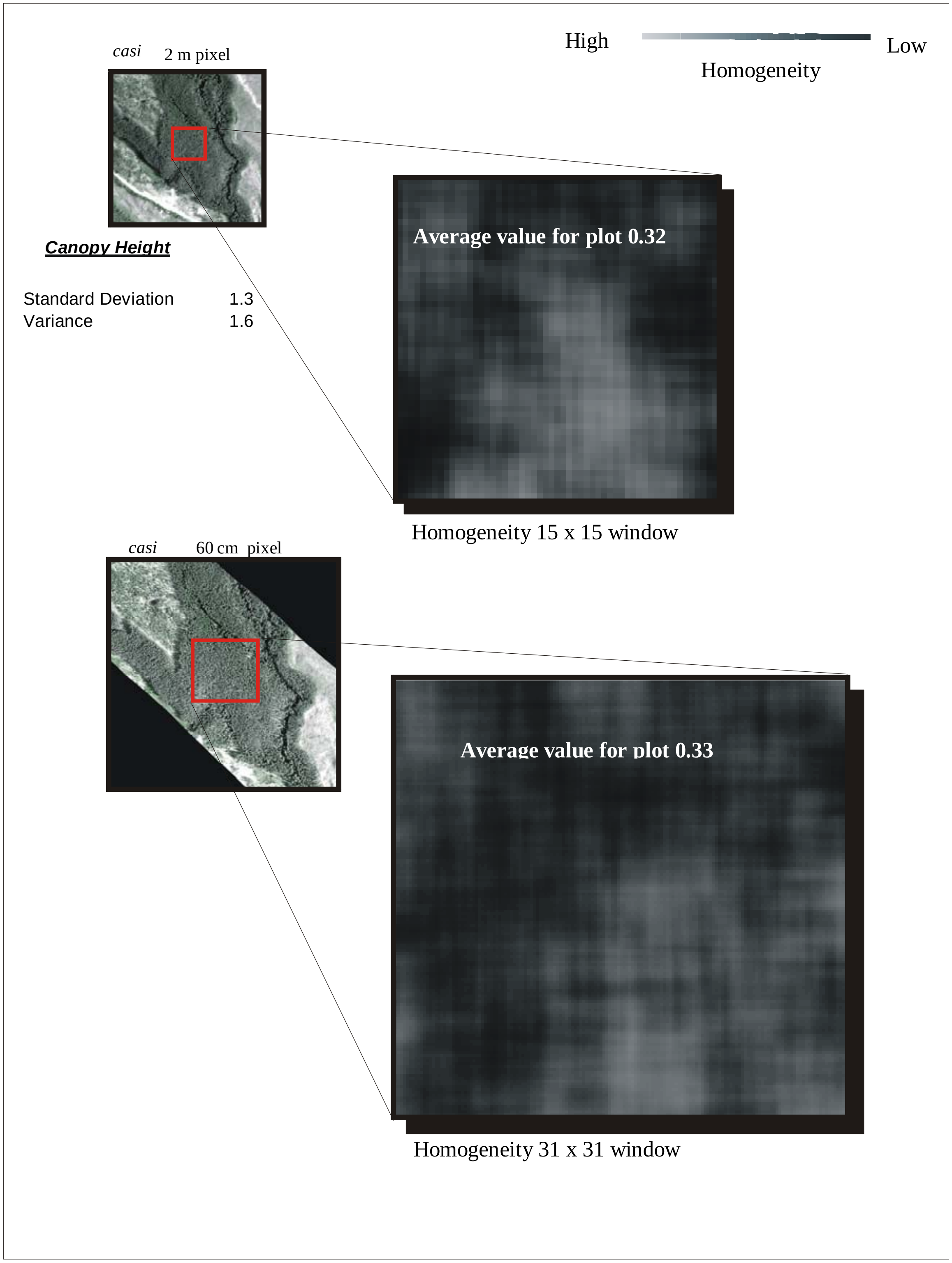

Example 5 – NDVI and Leaf Area Index

Reflectance properties of photosynthetic plants detected by multi-spectral remote sensors form the basis for vegetation indices; in turn, offering estimates of the type and quantity of vegetation on the ground. Healthy leaves absorb red and blue light, capturing energy for photosynthetic reactions. In addition, healthy leaves reflect near-infrared light as a function of their water content and cellular structure. Often input as information for classification purposes, the Normalized Difference Vegetation Index (NDVI) is established on these reflective properties of leaves. The NDVI is the difference between near-infrared and red reflectance, normalized by the sum of the reflectance of these wavelength bands. Besides species composition, factors that affect NDVI values include leaf morphology, leaf position on the tree (sunlit vs. shade), brightness of incoming sunlight, vegetation stress, and biomass. Although the relationships between these factors and NDVI are complex, certain associations are strong and useful for image interpretation.

As an example of differences among stand types in the Kananaskis study area, a deciduous, a mixedwood and a coniferous forest stand are identified based on information obtained in the field. Differences in reflectance properties of these stands are directly observable in the CASI 60 cm false colour and the derived NDVI imagery (Figure 9.11). From sub-scenes taken at the locations identified in Figure 9.11, the mean NDVI is calculated for a 16.8 square meter area of each stand type (Figure 9.12). The deciduous stand has the highest mean NDVI and lowest standard deviation (0.9; 0.081), followed by the mixedwood stand (0.81; 0.104) and the conifer stand (0.71; 0.191). The higher mean NDVI of the deciduous stand is due to aspen having broader leaves at the apex with relatively higher water content, and higher rates of photosynthesis than do the conifers at the time the image was captured.

Leaf area index (LAI) is the ratio of leaf to ground area. A high LAI corresponds to a large vegetative biomass. Among stands of a given species in similar environmental conditions, higher NDVI values are associated with higher LAI values. However, the relationship between NDVI and LAI is not linear; the rate of change in LAI decreases as NDVI values increase (Figure 9.13). As a general rule, the curve levels off (becomes saturation) when LAI is greater than 4. Furthermore, the relationship between NDVI and LAI depends on species composition; on the whole, deciduous stands have higher NDVI to LAI ratios than coniferous stands due to differences in leaf morphology, leaf angle and canopy structure.

As an example of the relationship between NDVI and LAI, two of the AFBMP Foothills pilot sites with similar species composition are compared. LPY (young Lodgepole pine) has a 3.5% lower NDVI (0.72) than does pilot site LPM (mature Lodgepole pine) (NDVI = 0.79) with estimated LAI values of 3.6 and 4.1, respectively (Figure 9.13). For forest biodiversity monitoring, empirical relationships can be established between LAI and NDVI for dominant species and, combined with species classification, used to predict LAI in stands within the monitored area as a whole.

Figure 10.11 CASI False Colour and NDVI Images - Kananaskis Study Area

casi false colour composite

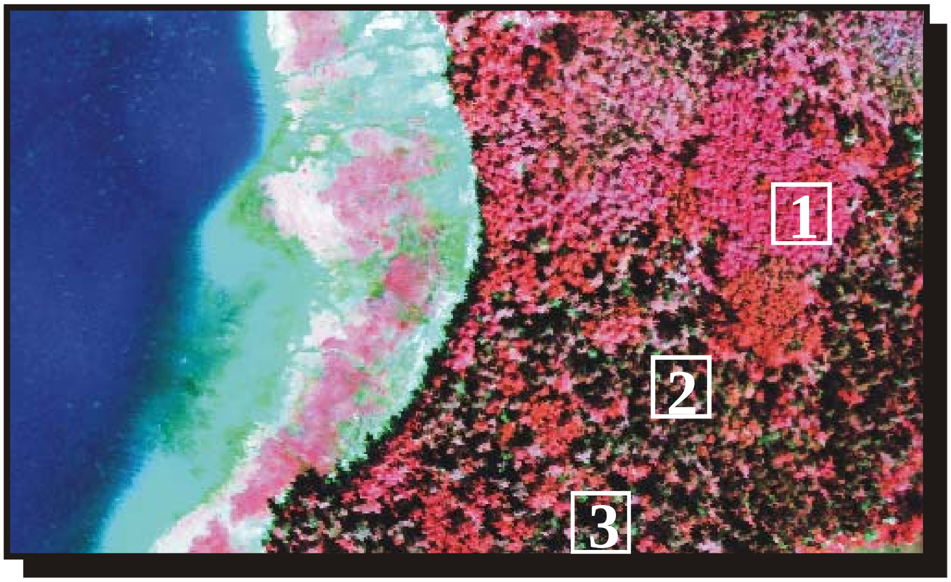

NDVI image

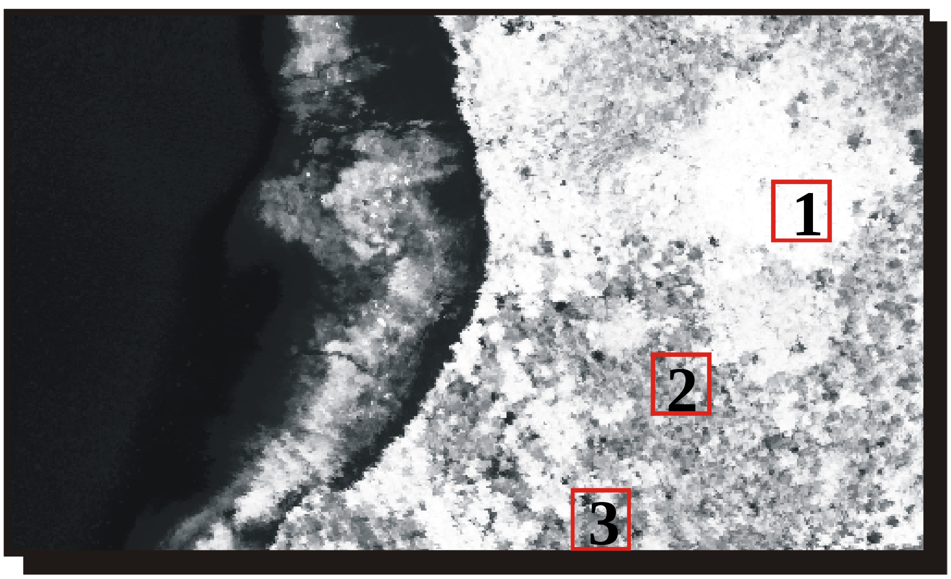

1. Decidious
2. Mixedwood
3. Coniferous

Along with other forest stand parameters, LAI estimates can be used to model actual and potential productivity, important biodiversity elements of forest stands.

As a ratio, the NDVI partially compensates for uneven illumination; reflectance values of both the red and near-infrared bands are similarly lowered in proportion to the depth of the shadow. Thus, using a NDVI image band lessens the strong shadow effects that influence texture when using a near-infrared band alone (see Example 4).

Figure 9.12 CASI False Colour and NDVI Images - Kananaskis Study Area Deciduous, Mixedwood and Coniferous Stands

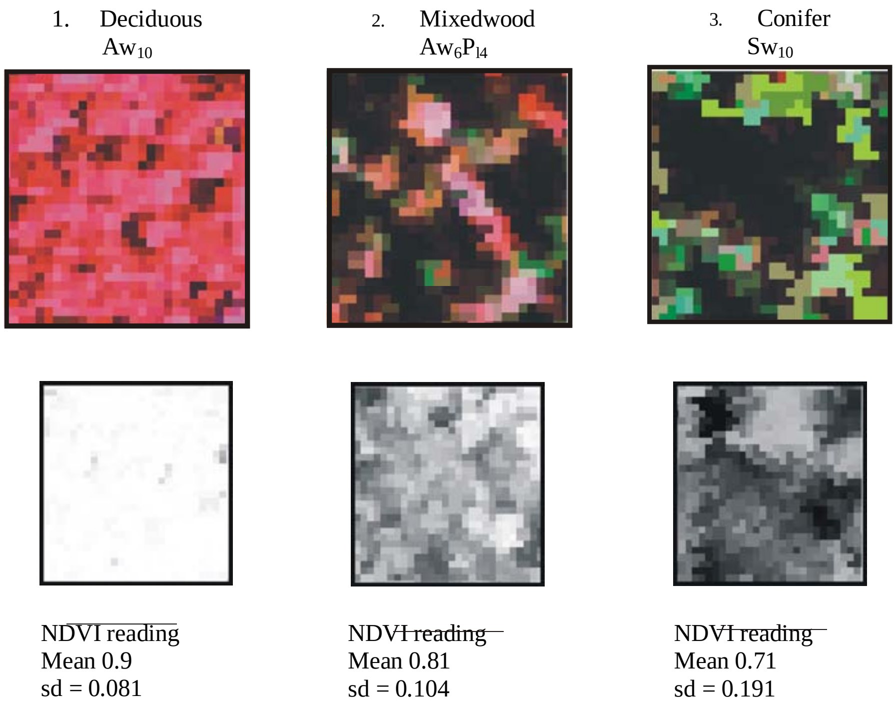

Figure 9.13 NDVI and Leaf Area Index - Foothills Pilot Sites: a) Lodgepole Pine Young (LPY) and b) Lodgepole Pine Mature (LPM)

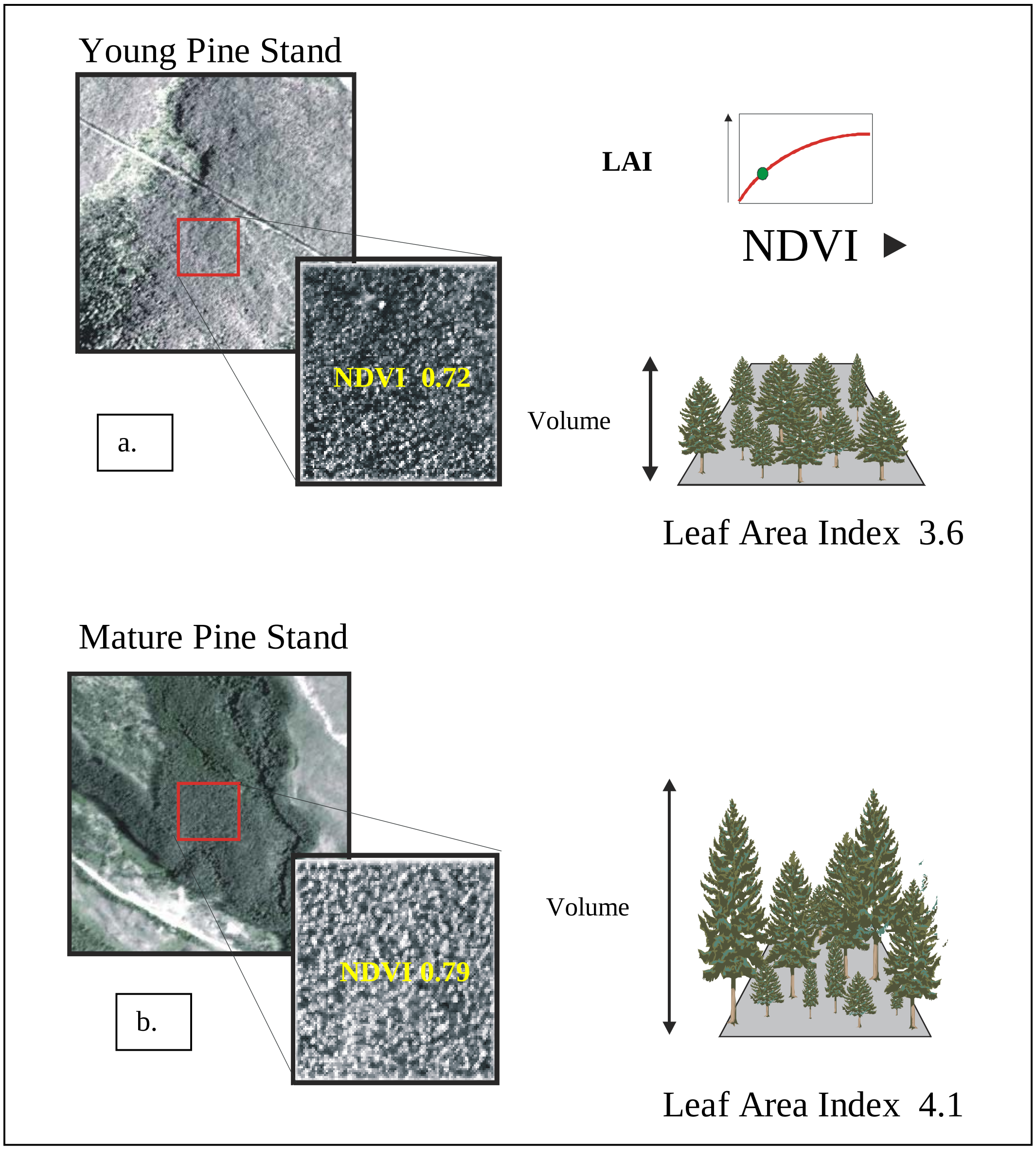

Conclusion and Recommendations

This chapter has examined and illustrated the use of high-resolution airborne imagery in forest biodiversity monitoring in Alberta. A remote sensing protocol, which describes the specific steps and choices that must be made in implementing this monitoring component is based on these examples and our review of the literature. It is important to note that this chapter contains only the high spatial resolution (small area covered) protocol; Chapter 8 details the specific recommendations on the use of low and medium spatial detail remote sensing imagery preceded this report.

Recommendation 1: Nine separate groups of biodiversity elements are recommended at various time scales for selected study sites within forest stands of the province (species composition, number of trees, canopy roughness, crown closure, NDVI, vegetation stress, LAI, canopy volume, and patch metrics). These groups contain all of the structural and process-related functions of forest ecosystems that can be reliably monitored by remote sensing and verified by ground observations in a realistic procedure.

Recommendation 2: To accomplish the monitoring of the nine groups of biodiversity elements at multiple spatial scales, high spatial resolution airborne (e.g., CASI or equivalent) or satellite (e.g., IKONOS or equivalent) imagery is required. We recommend that the biodiversity monitoring sites be prioritized and imagery be acquired as the priorities suggest (such as high priority areas being monitored annually).

Recommendation 3: The imagery must be calibrated to reflectance using the best available scene-dependent empirical methods; such corrections must account for atmospheric, topographic and radiometric (e.g., view angle) effects. Imagery must be geometrically correct.

Recommendation 4: Field data must be acquired to generate classification training data and for a variety of analytic and verification purposes (including regression and change accuracy assessment). Field protocols should include the accurate recording of plot boundaries, tree plot maps, tree species at each canopy stratum (emergent, medium, tallest), diameter at breast height (DBH), tree height, tree age, canopy closure, and leaf health.

Recommendation 5: Based on classification, object identification, and regression data, a change detection procedure to detect and identify change is required. The recommended approach is that baseline information be used to compare image data in subsequent years; only those areas exceeding a certain threshold would be flagged and checked in the field.

Acknowledgements

The authors thank Dr. Dan Farr of the Foothills Model Forest and Dr. Ron Hall of the Canadian Forest Service for their insights and contributions into the remote sensing pilot project. We are grateful for the field support provided by Phil Lee, Kelly Sturgess, Steve Hanus, Lindsay Tomyn and Jennifer Joy, and ARC, Vegreville, and by Deidre Davidson and Ryan Johnson, University of Lethbridge. In addition, the authors greatly appreciate the funds and support provided by the NRCan Science and Technology Internship Program, the Foothills Model Forest and the Canadian Forest Service. The space and support provided by the University of Calgary is also acknowledged and appreciated.

References

Adams, M. L., W. D. Philpot, and W. A. Norvell. 1999. Yellowness index: an application of spectral second derivatives to estimate chlorosis in leaves in stressed vegetation. *International Journal of Remote Sensing* 20 (18): 3663-3675.

Ahern, F., J. Sirois, W. D. McColl, R. P. Gauthier, T. T. Alfoldi, W. H. Patterson, and T. A. Erdle. 1991. Progress towards improved aerial defoliation survey methods by using electronic images. *Photogrammetric Engineering and Remote Sensing* 57: 187-194.

Bolduc, P., K. Lowell, and G. Edwards. 1999. Automated estimation of localized forest volume from large-scale aerial photographs and ancillary cartographic information in a boreal forest. *International Journal of Remote Sensing* 20(8): 3611-3624.

Brandtberg, T. 1998. Algorithms for structure- and contour-based tree species classification using digital image analysis. In *Automated Interpretation of High Spatial Resolution Digital Imagery for Forestry*. Victoria, British Columbia, February 10-12, 1998. D. A. Hill and D. G. Leckie, editors. Natural Resources Canada, Canadian Forest Service, Pacific Forestry Centre, Victoria, British Columbia. Pp. 199-207.

Chen, Z., C. D. Elvidge, and D. P. Groeneveld. 1999. Vegetation change detection using high spectral resolution vegetation indices. In *Remote Sensing Change Detection: Environmental Monitoring Methods and Applications*. R. S. Lunetta and C. D. Elvidge, editors. Sleeping Bear Press, Inc., Taylor & Francis Ltd. London.

Dikshit, O. and D. P. Roy. 1996. An empirical investigation of image resampling effects upon the spectral and textural supervised classification of a high spatial resolution multispectral image. *Photogrammetric Engineering and Remote Sensing*, 62 (9): 1085-1092.

Dickson, E. E., S. E. Franklin, and L. M. Moskal. 2000. Monitoring of forest biodiversity using remote sensing: Regional landscape (medium and low spatial resolution) protocol and examples. Alberta Forest Biodiversity Program Technical Report 4, Part 1.

Dralle, K. and M. Rudemo. 1996. Stem number estimation by kernel smoothing of aerial photos. *Canadian Journal of Forest Research*. 26:1228-1236.

Dralle, K. and M. Rudemo. 1997. Automatic estimation of individual tree positions from aerial photos. *Canadian Journal of Forest Research* 27: 1728-1736.

Eldridge, N. R. and G. E. Edwards. 1993. Continuous tree class density surfaces derived from high resolution airborne images. *GIS '93: Eyes on the Future, Vancouver, Canada*, pp. 947-954, Feb. 15-18, (Vancouver, Canada: Polaris Conferences).

Franklin, S. E., W. W. Bowers, and G. Ghitter. 1995a. Discrimination of adelgid-damage on single balsam fir trees with aerial remote sensing data. *International Journal of Remote Sensing*, 16(15): 2779-2794.

Franklin, S. E., R. H. Waring, R. W. McCreight, W. B. Cohen, and M. Fiorella. 1995b. Aerial and satellite sensor detection and classification of western spruce budworm defoliation in a subalpine forest. *Canadian Journal of Remote Sensing* 21(3): 299-308.

Franklin, S. E., M. B. Lavigne, M. J. Deuling, M. A. Wulder and E. R. Hunt. 1997. Estimation of forest Leaf Area Index using remote sensing and GIS data for modelling net primary production. *International Journal of Remote Sensing* 18(16): 3459-3471.

Franklin, S. E. and E. E. Dickson. 1999. Approaches for monitoring landscape composition and pattern using remote sensing. In Farr, D. R., S. E. Franklin, E.E. Dickson, G. Scrimgeour, S. Kendall, P. Lee, S. Hanus, N. N. Winchester and C. C. Shank, *Monitoring forest biodiversity in Alberta: Program framework. Alberta Forest Biodiversity Monitoring Program Technical Report 3*. Draft Report.

Franklin, S. E., R. J. Hall, L. M. Moskal, A. J. Maudie, and M. B. Lavigne. 2000. Incorporating texture into classification of forest species composition from airborne multispectral images. *International Journal of Remote Sensing*, 21: (1): 61-79.

Gerylo, G., R. J. Hall, S. E. Franklin, A. Roberts, and E. J. Milton. 1998. Hierarchical image classification and extraction of forest species composition and crown closure from airborne multispectral images. *Canadian Journal of Remote Sensing*, 24(3): 219-232.

Gougeon, F. A. 1995a. Comparison of possible multispectral classification schemes for tree crowns individually delineated on high spatial resolution MEIS images. *Canadian Journal of Remote Sensing* 21(1): 1-9.

Gougeon, F. A. 1995b. A crown-following approach to the automatic delineation of individual tree crowns in high spatial resolution aerial images. *Canadian Journal of Remote Sensing* 21(3): 274-284.

Gougeon, F. A. 1997. A locally adaptive technique for forest regeneration assessments from high resolution aerial images. Presented at the 19th Canadian Remote Sensing Symposium, May 24-30, 1997, Ottawa, Canada.

Gougeon, F. A., D. G. Leckie, D. Paradine, and I. Scott. 1998. Individual tree crown species recognition: The Nahmint study. In *Automated Interpretation of High Spatial Resolution Digital Imagery for Forestry*. Victoria, British Columbia, February 10-12, 1998. D. A. Hill and D. G. Leckie, editors. Natural Resources Canada, Canadian Forest Service, Pacific Forestry Centre, Victoria, British Columbia. Pp. 209-223.

Key, T., T. A. Warner, J. McGraw, and M. A. Fajvan. 1998. An evaluation of the relative value of spectral and phenological information for tree crown classification of digital images in the eastern deciduous forest. In *Automated Interpretation of High Spatial Resolution Digital Imagery for Forestry*. Victoria, British Columbia, February 10-12, 1998. D. A. Hill and D. G. Leckie, editors. Natural Resources Canada, Canadian Forest Service, Pacific Forestry Centre, Victoria, British Columbia. Pp. 243-254.

Lahde, E., O. Laiho, Y. Norokorpi, and T. Saksa. 1999. Stand structure as the basis of diversity index. *Forest Ecology and Management* 115: 213-220.

Larsen, M. 1998. Finding an optimal match window for spruce top detection based on an optical tree model. In *Automated Interpretation of High Spatial Resolution Digital Imagery for Forestry*. Victoria, British Columbia, February 10-12, 1998. D. A. Hill and D. G. Leckie, editors. Natural Resources Canada, Canadian Forest Service, Pacific Forestry Centre, Victoria, British Columbia. Pp. 55-66.

Leckie, D., X Yuan, D. S. Ostaff, H. Piene, and D. A. MacLean. 1992. Analysis of high resolution multi-spectral MEIS imagery for spruce budworm damage assessment on a single tree basis. *Remote Sensing of Environment* 40: 125-136.

Leckie, D. G., C. Jay, D. Paradine, and R. Sturrock. 1998. Preliminary assessment of *Phellinus weirii* infected (laminated root rot) trees with high resolution casi imagery. In *Automated Interpretation of High Spatial Resolution Digital Imagery for Forestry*. Victoria, British Columbia, February 10-12, 1998. D. A. Hill and D. G. Leckie, editors. Natural Resources Canada, Canadian Forest Service, Pacific Forestry Centre, Victoria, British Columbia. Pp. 187-195.

Lucas, N. S., P. J. Curran, S. E. Plummer, and F. M. Danson. 2000. Estimating the stem carbon production of a coniferous forest using an ecosystem simulation model driven by the remotely sensed red edge. *International Journal of Remote Sensing* 21(4): 619-631.

Lunetta, R. S. 1999. Applications, project formulation, and analytical approach. In *Remote Sensing Change Detection: Environmental Monitoring Methods and Applications*. R. S. Lunetta and C. D. Elvidge, editors. Sleeping Bear Press, Inc., Taylor & Francis Ltd. London.

Magnussen, S. and P. Boudewyn. 1998. Obtaining volume estimates from casi images of a thinning and fertilization trail. In *Automated Interpretation of High Spatial Resolution*

Digital Imagery for Forestry. Victoria, British Columbia, February 10-12, 1998. D. A. Hill and D. G. Leckie, editors. Natural Resources Canada, Canadian Forest Service, Pacific Forestry Centre, Victoria, British Columbia. Pp. 297-308.

Moskal, L. M. 1999. *AVI multilayer forest classification using airborne image texture*. Unpublished MSc Thesis, Department of Geography, University of Calgary.

Noss, R. F. 1998. At what scale should we manage biodiversity? In *Policy and Practices for Biodiversity in Managed Forests: The Living Dance*. F. L. Bunnell and J. F. Johnson, editors. UBC Press, Vancouver, BC.

Peterson, E. B. and N. M. Peterson. 1992. *Ecology, management, and use of aspen and balsam poplar in the prairie provinces, Canada*. Forestry Canada, Northwest Region, Northern Forestry Centre, Edmonton, Alberta. Special Report 1.

Pollack, R. 1998. Individual tree recognition based on a synthetic tree crown image model. In *Automated Interpretation of High Spatial Resolution Digital Imagery for Forestry*. Victoria, British Columbia, February 10-12, 1998. D. A. Hill and D. G. Leckie, editors. Natural Resources Canada, Canadian Forest Service, Pacific Forestry Centre, Victoria, British Columbia. Pp. 25-34.

Preston, R. A., D. S. Culvenor, and N. C. Coops. 1998. Modeling of tree species and structural attributes from high resolution multi-spectral imagery using decision tree analysis for east coast eucalypt forests of Australia.

Spanner, M. A., W. Acevedo, K. W. Teuber, and S. W. Running. 1984. Remote sensing of the leaf area index of temperate coniferous forests. Proceedings of 1984 Machine Processing of Remotely Sensed Data Symposium, 12-14 June (West Lafayette, IN, Purdue University), pp. 362-369.

St. Onge, B. A. and F. Cavayas. 1997. Automated forest structure mapping from high resolution imagery based on directional semivariogram estimation. *Remote Sensing and Environmen*t 61:82-95.

Reich, R. W. and R. Price. 1998. Detection and classification of forest damage caused by tomentosus root rot using an airborne multispectral imager (casi). In *Automated Interpretation of High Spatial Resolution Digital Imagery for Forestry*. Victoria, British Columbia, February 10-12, 1998. D. A. Hill and D. G. Leckie, editors. Natural Resources Canada, Canadian Forest Service, Pacific Forestry Centre, Victoria, British Columbia. Pp. 179-185.

Running, S. W., D. L. Peterson, M. A. Spanner, and K. B. Teuber. 1986. Remote sensing of coniferous forest leaf area. *Ecology* 67: 273-276.

Running, S. and E. R. Hunt. 1993. Generalization of a forest ecosystem model for other biomes, BIOME-BGC, and an application for global-scale models, In *Scaling Physiological Processes: Leaf to Globe*, Academic Press, pp. 141-157.

Wulder, M. 1999. Image spectral and spatial information in the assessment of forest structural and biophysical data. In *Automated Interpretation of High Spatial Resolution Digital Imagery for Forestry*. Victoria, B. C., Canada, February 10-12, 1998. Natural Resources Canada, Canadian Forest Service, Pacific Forestry Centre, Victoria, B. C. pp. 267-281.

Yuan, X., D. King, and J. Vlcek. 1991. Sugar maple decline assessment based on spectral and textural analysis of multispectral aerial videography. *Remote Sensing of Environment* 37: 47-54.